

44-11-412

MASSACHUSETTS INSTITUTE OF TECHNOLOGY  
ARTIFICIAL INTELLIGENCE LABORATORY

and

CENTER FOR BIOLOGICAL INFORMATION PROCESSING  
WHITAKER COLLEGE

A.I. Memo 787  
C.B.I.P. Paper 006

March, 1984

**A Theoretical Analysis of the Electrical Properties of a X-cell in the Cat's LGN:  
Does the Interneuron Gate the Visual Input to the X-System?**

**Christof Koch**

Electron-microscopic studies of relay cells in the lateral geniculate nucleus of the cat have shown that the retinal input of X-cells is associated with a special synaptic circuitry, termed the spine-triad complex. The retinal afferents make an asymmetrical synapse with both a dendritic appendage of the X-cell and a geniculate interneuron. The interneuron contacts in turn the same dendritic appendage with a symmetrical synaptic profile. The retinal input to geniculate Y-cells is predominately found on dendritic shafts without any triadic arrangement. We explore the integrative properties of X- and Y-cells resulting from this striking dichotomy in synaptic architecture. The basis of our analysis is the solution of the cable equation for a branched dendritic tree with a known somatic input resistance. Under the assumption that the geniculate interneuron mediates a shunting inhibition, activation of the interneuron reduces very efficiently the excitatory post-synaptic potential induced by the retinal afferent *without* affecting the electrical activity in the rest of the cell. Therefore, the spine-triad circuit implements the analog of an AND-NOT gate, unique to the X-system. Functionally, this corresponds to a presynaptic, feed-forward type of inhibition of the optic tract terminal. Since Y-cells lack this structure, inhibition acts globally, reducing the general electrical activity of the cell. We propose that geniculate interneurons gate the flow of visual information into the X-system as a function of the behavioral state of the animal, enhancing the center-surround antagonism and possibly mediating reciprocal lateral inhibition, eye-movement related suppression and selective visual attention.

© Massachusetts Institute of Technology, 1984

This report describes research done within the Artificial Intelligence Laboratory and the Center for Biological Information Processing (Whitaker College) at the Massachusetts Institute of Technology. The Center's support is provided in part by the Sloan Foundation and in part by the Whitaker College.

## 1. Introduction

It has long been recognized that the thalamus represents more than a mere relay-station for sensory signals between the periphery and the cortex. In fact, several properties make it very likely that the thalamus is a major pre-processing center for sensory information, enhancing or suppressing information before it reaches the cortex. Almost all sensory input to the cortex, with the exception of the olfactory system, passes through thalamic nuclei before it reaches the corresponding cortical areas for further processing. Morphological studies show an extremely complicated intrinsic circuitry that is just beginning to be unraveled. The most intriguing finding concerning the thalamus, however, is that it integrates a host of extrasensory signals. Considering only the visual system of the cat as we will do in this study, anatomical and physiological studies reveal that the dorsal part of the lateral geniculate nucleus (LGN) receives a very large, topographical projection from the visual cortex (Jones and Powell, 1969b; Gilbert and Kelly, 1975) and smaller projections from the thalamic reticularis nucleus (Minderhoud, 1971; Ohara, Sefton and Lieberman, 1980) including the perigeniculate (Lindstrom, 1982; Schmielau, 1979) and the midbrain reticular formation (Singer, 1977) including the locus coeruleus (Nakai and Takaori, 1974; Ahlsen and Lo, 1982) and the raphe nuclei (Ahlsen and Lo, 1982). The variety of extraretinal afferents is emphasized by the fact that only about 20% of the synaptic contacts in the LGN are formed by retinogeniculate fibers, while 45% are formed by corticofugal fibers and 35% by interneurons (Guillery, 1969b). The LGN seems therefore to be in a very strategic location to regulate the transmission of visual evoked signals to the cortex. The range of possible functions prescribed to it has correspondingly been very wide. It has been implicated in sharpening the center-surround antagonism (Hubel and Wiesel, 1961; Bullier and Norton, 1979; Ahlsen, Grant and Lindstrom, 1982), saccadic suppression (Noda, 1975a,b; Tsumoto and Suzuki, 1976), visual pattern masking (Breitmeyer and Ganz, 1976), lateral inhibition (Singer and Bedworth, 1973; Singer, 1977; Dubin and Cleland, 1977), binocular depth perception (Richards, 1968; Schmielau and Singer, 1977), increasing the Y-to-X cell ratio (Friedlander, Lin, Stanford and Sherman, 1981; Sherman, 1984) and gating as a function of visual attention and arousal (Meulders and Godfraind, 1969; Coenen and Vendrik, 1972; Singer 1973 and 1977). Moreover, the thalamic reticular nucleus, a structure closely related to the LGN, has been proposed to control selective visual attention by its action upon LGN cells (Yingling and Skinner, 1977; Crick, 1984; see also Koch and Ullman, 1984).

Ever since the early recordings by Hubel and Wiesel (1961), it has been recognized that while the receptive fields of geniculate neurons are concentrically organized—resembling retinal ganglion cells—inhibition seems to play a greater role in the LGN than in the retina (Sillito and Kemp, 1983). The degree of inhibition seems to be influenced by a wide variety of parameters, including eye movements, retinal activity and the state of wakefulness of the

animal. It has been suggested (Dubin and Cleland, 1977), that intergeniculate interneurons are involved in a precise, spatially organized inhibition while neurons in the perigeniculate are part of a more general, diffuse inhibitory system that modulates LGN excitability. Recently, EM reconstructions of physiological identified and stained geniculate neurons have shown, that the so-called spine-triad complex is predominately found on X-relay cells (Wilson, Friedlander and Sherman, 1984; Hamos *et al.*, 1984a,b). In this report we study the electrical properties of reconstructed geniculate X- and Y-cells on the basis of 1-dimensional cable theory. We argue—supported by computer simulations—that this circuit could be the site of a very localized AND-NOT type of veto operation, functionally equivalent to presynaptic inhibition. The geniculate interneuron, contributing the inhibitory synapse to the spine-triad circuit, therefore controls the flow of visual information into the X-system. The interneuron, in turn, receives input from the visual cortex, the midbrain and the thalamic reticular nucleus and thus integrates information from a variety of sources. This hypothesis helps understanding a large number of studies reporting widely differing effects of inhibition in geniculate X- and Y-cells (Singer and Bedworth, 1973; Noda, 1975a,b; Tsumoto and Suzuki, 1976; Fukuda and Stone, 1976; Foote *et al.*, 1977; Derrington and Fuchs, 1979; Bullier and Norton, 1979; Berardi and Morrone, 1984). We argue that the interneuron-mediated inhibition enhances the center-surround antagonism and may underly reciprocal lateral inhibition, eye-movement related suppression and, in particular, *selective visual attention*.

The paper is divided into three main parts. In the next section we will provide a brief anatomical description at the light- and electron-microscopy level of geniculate neurons. In the second part (sections 3, 4 and 5) we describe the methods used in the course of our analysis and present the results of our model calculations for the electrical properties of a geniculate X-cell, carefully examining the underlying assumptions of passive, one-dimensional cable theory. In the last part (section 6), we discuss the physiological evidence in favor of the vetoing mechanism and examine some of the functional implications of our results in the light of the circuitry of the LGN and its afferents.

## 2. The Morphology and Synaptology of Geniculate Cells

### 2.1 The Morphology of Projection Neurons

In recent years several laboratories have provided evidence of a structure-function relationship for cat geniculate neurons. Most of these classifications can be traced to Guillery's studies using Golgi impregnated cells (1966, 1969a,b). More recently, Friedlander,

Lin, Stanford and Sherman (1981; see also Friedlander, Lin and Sherman, 1979) used intracellularly injected horseradish peroxidase (HRP) and physiological identification to classify geniculate cells. Geniculate X and Y relay-cells can be distinguished from each other by purely morphological criteria, similar to retinal X- and Y-ganglion cells (Boycott and Wassle, 1974). The main characteristics are (see figure 1):

- X-cell dendrites always remain within a single lamina, whereas *all* Y-cells have dendrites that cross laminar boundaries.
- Y-cells have both larger somata and thicker axons than X-cells.
- X-cells tend to be oriented perpendicular to the lamination, while Y-cells tend to have radially symmetric dendritic trees.
- Y-cells tend to have only a few and simple dendritic appendages found near branching points, whereas X-cells usually have complex stalked processes.

A large number of both X- and Y-cells have axon collaterals in the perigeniculate, although more Y- than X-cell axons do. Similarly, X-cell axons tend to make axon collaterals within the geniculate lamina, while fewer Y-cell axons do. This data suggests that differences in the X- and Y-pathways are not determined uniquely in the retina, but also occur in the LGN.

## 2.2 The Geniculate Interneuron

Geniculate interneurons, i.e. neurons without axon projecting to the cortex, are usually associated with Guillery's class 3 cells (LeVay and Ferster, 1979; Hamos, van Horn, Raczkowski, Uhrich and Sherman, 1984). These cells have the smallest somata with very fine, sinuous dendrites oriented orthogonal to the lamination and do not show an axon leaving the LGN (see figure 1). An heterogeneous assortment of appendages, many quite complicated in appearance and often connected to dendrites by long stalks, can be found all along the dendrites (Guillery, 1966).

One surprising result of Friedlander *et al.* (1981) is their observation of X-relay cells with class 3 morphology. Thus, either two subgroups of class 3 exist or geniculate interneurons, which are spiking, behave as both an inter- and projection-neuron; i.e. they locally form dendro-dendritic synapses while projecting at the same time to the cortex.

The ratio of projection cells to interneurons is uncertain due to electrode sampling biases. The data of Friedlander *et al.* (1981) seems to indicate that Y-cells represent roughly 35% of the neurons in the A-laminae, in agreement with Friedlander and Stanford (1984), while LeVay and Ferster (1979) report somewhat lower percentages. Estimates of the percentage of geniculate interneurons range from less than 10% (Lin, Kratz and Sherman, 1977) to

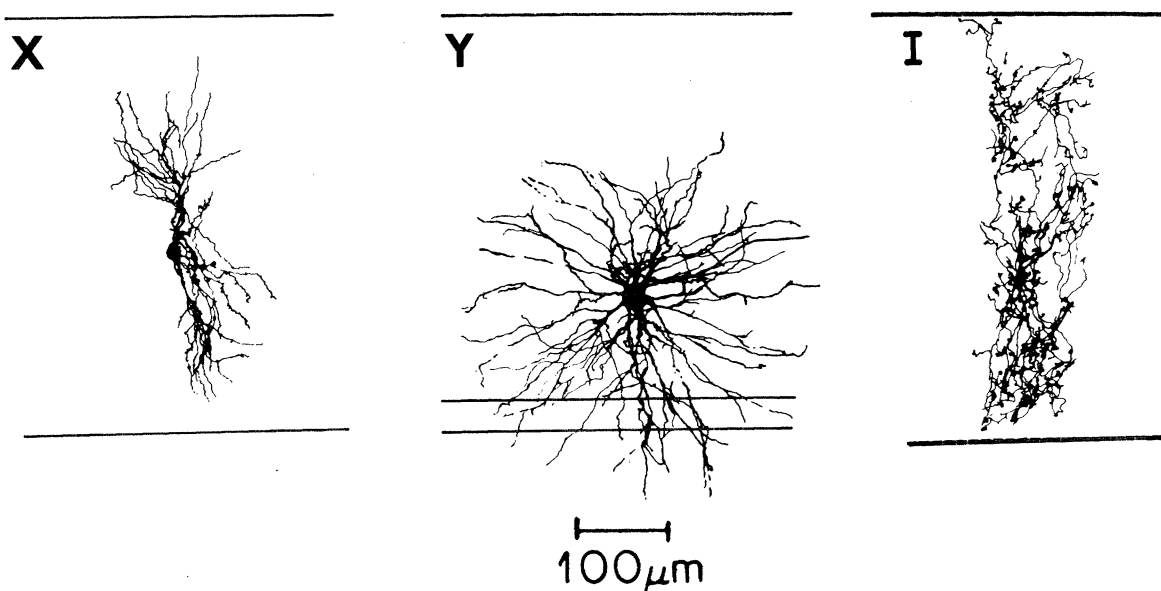


**Figure 1.** Drawing of a X-, Y- and a presumed interneuron in the dorsal LGN of an adult cat (see text). The interneuron could not be confirmed as a relay cell. Its morphology is very similar to the "local circuit" cell found by Hamos *et al.*, 1984b. Note its delicate, complex dendritic appendages, most likely presynaptic to processes of X-relay cells. The drawings were kindly provided by M. Friedlander.

roughly 25% (LeVay and Ferster, 1979; Fitzpatrick *et al.*, 1984). Thus, the ratio between Y-cells, X-cells and interneurons seems to be roughly 1:2:1. This is in striking contrast to the retina, where X-cells outnumber Y-cells by more than 10 to 1 (Wassle, Boycott and Illing, 1981; Wassle, Peichl and Boycott, 1981).

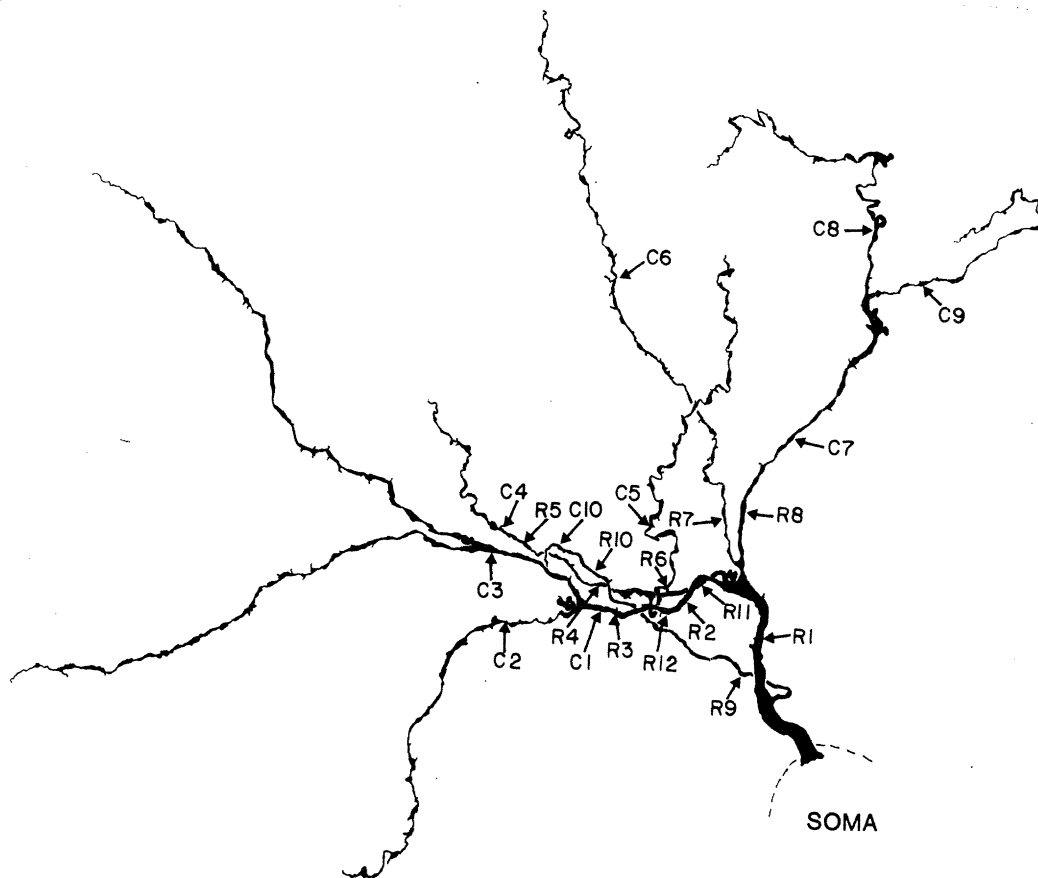
### 2.3 Synaptic Ultrastructure of Geniculate Neurons

Several studies have focused on the ultrastructure of geniculate relay cells, with special emphasis on the synaptic connections made by optic tract axons onto the geniculate cells (Jones and Powell, 1969b; Guillery, 1969a,b; Famiglietti, 1970; Wong, 1970; Famiglietti and Peters, 1972; Wilson, Friedlander and Sherman, 1984; Rapisardi and Miles, 1984). More recently, Hamos and colleagues identified and stained in an Herculean task a single optic tract axon originating from a retinal X-cell, serially sectioning and reconstructing a few of the postsynaptic neurons. (Hamos, Raczkowski, van Horn and Sherman, 1983; Hamos *et al.*,

1984). In the following we will briefly summarize these studies, adopting the nomenclature proposed by Guillery (1969a) to classify synaptic profiles in the LGN. RLP terminals, have round, large synaptic vesicles, asymmetrical contacts, contain pale mitochondria and are retinal in origin. RSD terminals, also have round synaptic vesicles and asymmetrical contacts, but the terminals are small and contain sometimes dark mitochondria. These synapses arise in most part from the massive corticogeniculate projection. F terminals, believed to be inhibitory, are characterized by flattened synaptic vesicles and symmetrical synaptic contacts. This class can be further subdivided. While F2 terminals arise from geniculate interneurons, most of the F1 terminals are undoubtedly from perigeniculate sources (see also Ohara, Sefton and Lieberman, 1980).

- X-cells receive the majority of their 200 to 400 retinal terminals onto dendritic appendages or spines. These appendages are usually found within  $100\mu m$  from the soma, are densely populated with mitochondria and frequently show a spine apparatus. Each of them has associated with it at least one, and in numerous cases several RLP terminals in addition to symmetrical F2 terminals (see figure 3). The retinal input is always associated with the *triadic arrangement*, whereby the retinal axon terminates on both a dendritic appendage of the relay cell and on a process of the interneuron. The interneuron in turn forms a F2 synapse onto the same appendage (figure 3). These triadic arrangements have also been described in primate's LGN (Hamori, Pasik, Pasik and Szentagothai, 1974). Part of the retinal input synapses directly onto the dendritic stem, with the F2 synapse close by. F2 terminals contribute a sizable fraction (10 – 20%) to the total synaptic count on distal dendrites, where no retinal inputs are present. F1 terminals are rarely seen on X-cells. RSD terminals are always in direct contact with the dendritic stem and rapidly become the predominant synaptic type only a few tens of microns from the soma. In fact, beyond  $100\mu m$  they constitute the only excitatory input to relay cells. Overall, RSD terminals outnumber RLP terminals by a factor 4 – 6.
- In Y-cells the majority of the 200 to 400 retinal synapses terminate on the dendritic stems, and only few synapse on dendritic appendages. Moreover, practically none of the retinal input is associated with triades. Inhibitory, F1 synapses, are distributed throughout the cell, terminating directly on the dendritic stem. The processes associated with the F1 synapses do not receive any local retinal input. The distribution and strength of the cortical input is similar to the X-cells.
- Much less is known about the cellular ultrastructure of the interneurons. The retinal input is either associated with triades or makes isolated terminals onto dendrites and the soma. Interneurons receive abundant F1 and RSD terminals.

In conclusion, the physiological X and Y classification of LGN cells seems to be reflected



25  $\mu$ m

**Figure 2.** Part of the HRP-stained and electrophysiologically identified X-cell used in our model calculations. The cell was made up of altogether four such dendritic trees. Synapses were placed onto the cell according to their known statistical distribution (see arrows). The locations of 10 dendritic appendages are indicated by R followed by a number, while the corticofugal synapses are marked by a C followed by a number. The drawing was kindly provided by S. Bloomfield.

in differing synaptic architectures. X-cells receive their retinal input onto special sites, with a distinct morphology and additional synaptic circuitry, whereas Y-cells are contacted in a direct fashion by the retinal input. Our analysis will be based on this striking dichotomy in the pattern of synaptic innervation.

### 3. Our Model of a Geniculate X-cell

We calculated the electrical properties of spines on the basis of measurements taken from HRP-stained cells and intracellular recordings. The morphological material used for our

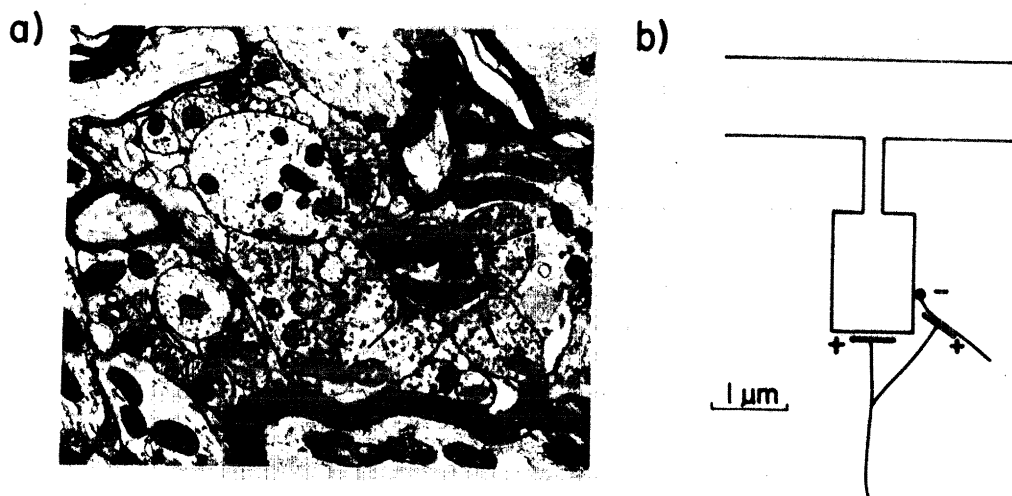


**Figure 3.** (a) EM picture of a typical dendritic appendage with associated triad arrangement on a X-cell. Note that the spine contains a high density of mitochondria. The two small arrows point to two RLP terminals presynaptic to the spine and the dendrite of the relay cell. The two large arrows indicate a F2 synapse. The synapse from the retinal afferent onto the interneuron occurs in a different section. (b) A schematic drawing of our model of the dendritic appendage. The diameter of the spine neck,  $d_N$ , usually set at  $0.2\mu\text{m}$ , was varied between  $0.1$  and  $0.4\mu\text{m}$ . The scale bar applies to both figures. The photograph was kindly provided by J.Hamos.

simulation was kindly provided by S. Bloomfield and M.Sherman. Briefly, their experimental protocol was as follows (Bloomfield and Sherman, 1984): Using HRP-filled microelectrodes (with dc-resistances ranging from  $70$  to  $120M\Omega$ ), cells in the A laminae of an adult cat's dorsal LGN were characterized extracellularly as either X- or Y-cells according to the usual criteria (Wilson *et al.*, 1984). After positive identification, the cell was impaled, its main physiological properties were confirmed, and the HRP was injected. The somatic input resistance  $K_{ss}$  was estimated from the voltage response following the injection of hyperpolarizing current pulses. Input resistances ranged between  $15$  and  $25M\Omega$ . After recovery of the HRP filled cells, camera-lucida drawings were constructed and the dimensions of the individual dendrites were measured, taking account of the three-dimensional extent of the dendritic arbor. The dendritic tree was approximated in terms of cylinders of appropriate length and diameter. Linear distances were corrected for the estimated amount of shrinkage caused by the HRP staining and montage, by multiplying their values by  $1.15$  (J.Hamos; personal communication). Our analysis will be based on the X-cell shown in figure 2. Because only one primary dendrite and its associated dendritic tree were reconstructed, we assumed that the dimension of the remaining three primary dendrites and their dendritic trees are similar.

The dendritic appendages were described using average dimensions as measured from EM



data kindly provided by J.Hamos (figure 3). A typical dendritic appendage was modeled by a thin cylinder, the spine neck,  $1.0\mu m$  long, and a variable diameter and by a thicker cylinder, the spine head,  $1.5\mu m$  long and  $1.0\mu m$  thick. The spine neck diameter was varied between  $0.1$  and  $0.4\mu m$ . We usually assumed a value of  $0.2\mu m$ . In accordance with the known distribution and total number of dendritic appendages (Wilson et al., 1984; Hamos et al., 1984), each of the four main dendritic trees carried 58 appendages, spaced  $8\mu m$  apart. Since appendages have not been reported beyond  $100 - 120\mu m$ , they were confined to dendrites no more than  $100\mu m$  away from the soma (see figure 2).

#### 4. Theoretical Considerations

##### 4.1 Linear Electrical Properties of the Dendritic Tree

We use one-dimensional cable theory to describe the electrical properties of a passive dendritic tree. The reader should consult Rall (1977) and Jack, Noble and Tsien (1975) for a review of classical cable theory and Koch, Poggio and Torre, (1982) and Koch and Poggio (1983a) for specific details regarding our computational methods. We will discuss in section 5.3 how our results change if significant membrane nonlinearities are introduced into the model. Under the assumption that the membrane does not contain any nonlinearities, the electrical properties of an arbitrary branched dendritic tree are completely captured by the complex transfer resistances  $\tilde{K}_{ij}(\omega)$  for any two locations  $i$  and  $j$  in the dendritic tree. A given current input at locations  $i$ ,  $I_i(t)$ , can be "propagated" by the associated  $K_{ij}(t)$ , the Fourier transform of  $\tilde{K}_{ij}(\omega)$ , to another location  $j$  to give the depolarization:

$$V_j(t) = K_{ij}(t) * I_i(t), \quad (1)$$

where  $*$  represent convolution. If the two locations  $i$  and  $j$  coincide, one obtains the familiar input impedance  $\tilde{K}_{ii}(\omega)$  seen by an electrode (for current injection) at that location. The direct current value  $\tilde{K}_{ij}(0)$  of the transfer function is the ohmic transfer resistance seen for steady-state current inputs:  $V_j = \tilde{K}_{ij}(0) \cdot I_i$ .

The algorithm used to determine the transfer function, an extension of an algorithm proposed by Butz and Cowan (1974), takes as input the branching structure, the length and the diameter of each dendritic segment (for details of the computer implementation see Koch and Poggio, 1984). It does not place any restriction on the geometrical structure of the dendritic tree nor on the diameter of the branches.

Since little is known about the passive electrical properties of geniculate neurons, we have to infer the cable parameters from physiological measurements. To estimate the value

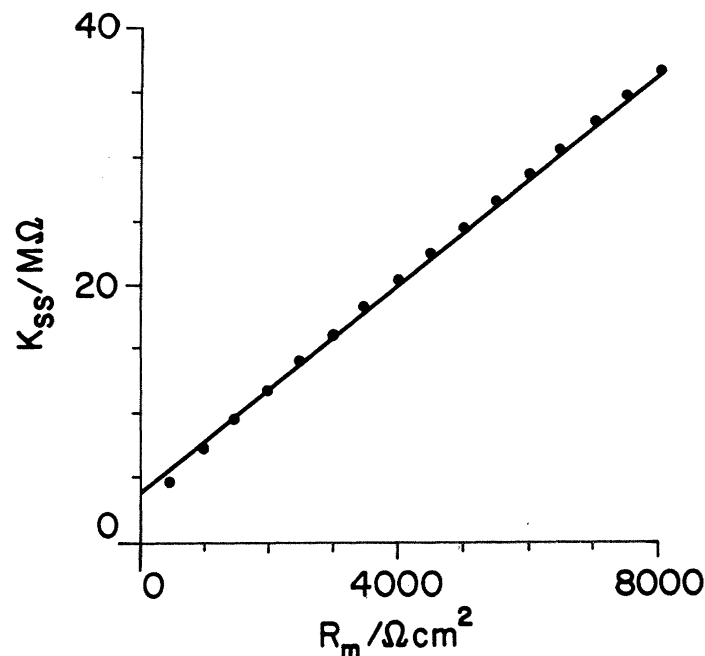


**Figure 4.** Calculated somatic input impedance  $K_{ss}$  for varying values of the membrane resistance  $R_m$ .  $R_m$  is assumed to be constant throughout the cell. The line is the best fit through the individual points ( $r^2 = 0.9993$ ). Such a linear relation between  $R_m$  and  $K_{ss}$  is predicted if the neuron can be described as equivalent cylinder (Rall, 1977).

of the membrane resistance  $R_m$  we computed the soma input resistance  $K_{ss}$ , under the assumption that  $R_m$  is constant throughout the cell. Figure 4 shows the resulting plot of  $K_{ss}$  as a function of  $R_m$ . The points clearly lie on a straight line, as expected if the neuron can be described by an equivalent tree (eq. (5.16) in Rall, 1977). For  $R_m = 4000 \Omega cm^2$  the somatic input resistance equals  $20.5 M\Omega$ , the midpoint of the experimental observed range of resistances for X-cells ( $20.6 \pm 3.0 M\Omega$ ; Bloomfield and Sherman, 1984). If not otherwise stated, we will use  $4000 \Omega cm^2$  throughout our analysis.

While the membrane resistance can vary over several orders of magnitude in different neuronal systems, values for the membrane capacity  $C_m$  do not vary over more than one order of magnitude (Brown, Perkel, Norris and Peacock, 1981). For a value of  $2 \mu F cm^{-2}$  throughout the cell, the membrane time constant  $\tau_m = R_m C_m$ , equals  $8 ms$ , a value at the lower end of the experimentally observed values ( $10.7 \pm 1.5 ms$ ; Bloomfield and Sherman, 1984).

The resistivity of the cytoplasm,  $R_i$ , usually lies between  $50$  and  $200 \Omega cm$  (Barrett, 1975). Owing to the presence of mitochondria and related organelles in the dendritic appendages (figure 3), which will tend to increase the intracellular resistance, we assume a value of  $200 \Omega cm$  for the spine cytoplasm and  $100 \Omega cm$  for the dendritic and somatic cytoplasm.

---

$i$	$j$	$K_{ij}$	
r11	r11	116.77	120.20
r11'	r11'	50.16	53.50
r11	soma	18.05	19.19
r11'	soma	18.05	19.19
r11	r12	22.29	25.28
r11	c5	44.75	50.62
c5	c5	139.59	152.76
c5	soma	16.37	18.42
soma	soma	20.59	20.57
tip	tip	320.7	349.1
tip	soma	15.01	17.74

**Table 1.** Representative values for some steady-state input- and transfer-resistances at various locations  $i$  and  $j$  throughout the cell shown in figure 2. The left column shows  $K_{ij}$  if  $R_m$  has the same value ( $4000\Omega cm^2$ ) throughout the cell. In the right column  $R_m$  equals  $800\Omega cm^2$  in the soma and the primary dendrites and  $10020\Omega cm^2$  elsewhere. The somatic input resistance is in both cases equal.  $r11'$  designates the location just below the spine, directly on the dendritic shaft. The row with *tip* indicates the average values measured at the tips of the 9 major dendritic terminal branches. Compare the values of dendritic input impedance ( $r11'$  and *c5*) with the  $103M\Omega$  measured by Jahnsen and Llinas (1984b) in presumed intradendritic recordings.

Approximating the electrotonic length of the geniculate cell by the sum of the electrotonic lengths of the individual branches weighted by the branch input conductance, yields  $L = 0.80$ . As shown by Segev and Rall (1983), this measure of  $L$ , rather than the simple average obtained by the equal weighting of the individual  $L_i$ 's, comes close to the value of  $L$  obtained by peeling the somatic decay transient (Rall, 1969).

Table 1 illustrates some typical input- and transfer-resistances as computed by our program. Note that the transfer resistance from the spine to the soma is equal to the transfer impedance from the dendritic shaft, directly below the spine, to the soma. This is due to the very small surface area of the dendritic appendage, minimizing current losses. Thus, as we have pointed out before (Koch and Poggio, 1983a,b), somatic depolarization due to a current input is the same, irrespectively of whether the synapse is on the spine or directly on the dendrite.

#### 4.2 Synaptic Inputs and their Properties

Synaptic inputs consist of transient conductance changes to specific ions and are not currents. Synaptic inputs effectively open "holes" in the membrane for ions with a reversal potential  $E_1$  measured with respect to the local resting potential  $V_{rest}$ . If the conductance for a specific ion changes by the amount  $g_1(t)$ , the induced potential change at the synapse

relative to the resting potential, is given by a Volterra-integral equation

$$V_1(t) = K_{11}(t) * \{g_1(t)(E_1 - V_1(t))\} \quad (2)$$

Since the retinal input activates many synapses simultaneously, as witnessed by the large number of synapses made by a single optic tract axon (Hamos *et al.* 1984), the interaction between different synapses has to be taken into account (Koch *et al.* 1982; Segev and Parnas, 1983).

Let us consider the case of an excitatory synapse at location  $e$  modulating the conductance change  $g_e(t)$  of an ionic species with equilibrium potential  $E_e > 0$  (relative to the resting potential) and an inhibitory synapse modulating the conductance change  $g_i(t)$  to an ionic species with equilibrium potential  $E_i < 0$  at location  $i$  (the locations  $i$  and  $e$  can coincide). For transient conductance inputs the system of coupled Volterra integral equations giving the resulting change in somatic potential is:

$$\begin{aligned} V_s(t) &= \{g_e(t)(E_e - V_e(t))\} * K_{es}(t) + \{g_i(t)(E_i - V_i(t))\} * K_{is}(t) \\ V_e(t) &= \{g_e(t)(E_e - V_e(t))\} * K_{ee}(t) + \{g_i(t)(E_i - V_i(t))\} * K_{ie}(t) \\ V_i(t) &= \{g_e(t)(E_e - V_e(t))\} * K_{ei}(t) + \{g_i(t)(E_i - V_i(t))\} * K_{ii}(t). \end{aligned} \quad (3)$$

For steady-state inputs, this reduces to a system of 3 coupled, algebraic equations. In the general case of  $n$  interacting synapses, the resulting  $n + 1$  algebraic equations can always be brought into the form  $AV = b$  and solved simply by inverting the matrix  $A$ . It can be proved for stationary synaptic inputs, that a shunting inhibitory synapse maximally suppresses the somatic depolarization, if it is on the *direct path* between the site of the excitatory synapse and the soma (Koch *et al.*, 1982; Koch, 1982). The specificity of this effect is such that if inhibition is not on the direct path, for instance  $20\mu m$  behind the excitatory synapse, on a dendrite branching off the direct path or on a spine, it will not be able to influence the evoked excitatory postsynaptic potential (EPSP) to any significant degree (Koch *et al.*, 1982, 1983). The strength of the nonlinear interaction between excitation and inhibition is maximal when the reversal potential of inhibition is equal or close to the resting potential of the cell (Torre and Poggio, 1978).

## 5. Results

In their analysis of cortical spines, Koch and Poggio (1983a,b) consider the electrical properties of the local circuit consisting of an excitatory and an inhibitory synapse on the

$g_e$	0.005	0.005	0.005	0.01	0.02	0.02	0.02	0.05	0.05
$g_i$	0.005	0.02	0.01	0.1	0.02	0.05	0.2	0.05	0.2
$r, i, c$	26.1	17.0	10.4	15.6	32.2	25.6	18.7	34.6	25.7
	26.5	14.2	3.87	6.85	30.5	19.0	6.44	13.0	13.2
$r, i$	16.2	7.64	2.01	3.85	20.0	11.9	3.91	21.1	8.63
	19.5	9.77	2.77	5.30	26.3	16.0	5.53	28.9	12.3
$c, i$	16.4	11.3	8.73	12.6	20.4	17.7	15.9	22.1	20.1
	14.6	6.33	1.21	1.88	12.5	5.72	11.2	7.85	1.60
$r, c$	35.1	35.1	35.1	40.9	44.9	44.9	44.9	47.8	47.8
	37.2	37.2	37.2	44.3	49.8	49.8	49.8	55.2	55.2
$r$	26.0	26.0	26.0	32.4	37.1	37.1	37.1	40.8	40.8
	29.9	29.9	29.9	39.0	46.8	46.8	46.8	54.1	54.1
$c$	25.1	25.1	25.1	31.4	36.2	36.2	36.2	40.2	40.2

**Table 2.** The somatic potential evoked by 30 synapses for varying steady-state conductance inputs. At each of the ten excitatory, retinal synapses, termed  $r$  ( $r_1$  through  $r_{10}$  of figure 2), conductance changes by  $g_e$  with  $E_e = 80mV$ . Each retinal synapse is associated with one inhibitory synapses, designated by  $i$ , with an associated conductance change  $g_i$  and  $E_i = 0mV$ . Ten excitatory, extraretinal synapses, termed  $c$  ( $c_1$  through  $c_{10}$  of figure 2), contact the dendrites directly (with  $g_e$  and  $E_e = 80mV$ ). Triads, i.e. retinal excitation and interneuron-mediated inhibition, are either located on the dendritic appendages (upper case) or are assumed to lie directly on the dendritic shaft, below the spine stem (lower case). The six rows show  $V_s$  in the case when all synapses are activated simultaneously ( $r, i, c$ ), only the synapses making up the triad ( $r, i$ ), the extraretinal synapses in the presence of inhibition ( $c, i$ ), the excitatory synapses ( $r, c$ ) and each of the excitatory synapses by themselves ( $r$  and  $c$ ). For the values of the neuronal parameters see Table 1.

same spine, a situation known to occur in mammalian cortex (Jones and Powell, 1969a; Scheibel and Scheibel, 1968; Famiglietti and Peters, 1972; Sloper and Powell, 1979). If the conductance change associated with the inhibitory synapse is above a critical value ( $\approx 0.05\mu S$ ), inhibition reduces the EPSP evoked by the excitatory synapse quite efficiently, without inhibiting electrical activity outside of the spine. We will examine the plausibility of this claim in the case of the spine-triad circuit, using physiologically characterized and anatomically reconstructed geniculate neurons.

### 5.1 Stationary Inputs

We computed the somatic potential for three different populations of synapses for various input amplitudes. Ten pairs of excitatory and inhibitory synapses were distributed on different dendritic appendages as shown in figure 2 (with conductance change  $g_e$  and  $g_i$ ).

An additional ten excitatory synapses (from corticofugal fibers) were placed directly on the dendritic stem in the distal half of the tree (with a conductance change  $g_e$ ). The strength of inhibition,  $g_i$ , was assumed to vary between 0.01 and  $0.2\mu S$ . The two sets of excitatory synapses have the same conductance change, varying between 0.005 and  $0.05\mu S$ . The actual size of the conductance change at a synapse is an open question, though a value between 0.01 and  $0.1\mu S$  is not unreasonable. For the sake of comparison, recall that a single ACh quantum at the neuromuscular junction induces a conductance change around  $0.06\mu S$  (Gage and McBurney, 1972), while GABA and glycine mediated conductance changes are larger than  $0.1\mu S$  (Ben-Ari, Krnjevic, Reiffenstein and Reinhardt, 1981; Gold and Martin, 1983). The reversal potential of all excitatory synapses is always fixed at  $80mV$ , relative to the resting potential.

Table 2 shows the result in the case of shunting inhibition, i.e.  $E_i = 0mV$ . Several conclusions can be drawn from these and similar results.

(i) Inhibition must be at least five times stronger than the excitation, before it reduces the retinal evoked depolarization to a substantial degree. In a lumped membrane circuit where excitation and inhibition coincide, the asymptotic ratio of somatic potential without inhibition to somatic potential in the presence of inhibition,  $F_{dc}$ , can be shown to be  $(g_i/g_e) + 1$  (Koch *et al.*, 1992).

(ii) Under these conditions, the retinal input will effectively be "switched" off, without inhibiting the cortical evoked depolarization in the rest of the cell. Even in the presence of a strong inhibition, at least 50% of the cortical evoked EPSP's will reach the soma.

(iii) If the triad is localized directly onto the dendrite, instead of onto the dendritic appendage, the interneuron-mediated inhibition will strongly reduce cortical evoked activity. It will be less efficient, however, in reducing the retinal-mediated excitation than before.

(iv) Under most circumstances, significant saturation occurs between excitatory synapses, reducing their synaptic efficiency. The sum of the individual somatic EPSP's induced by cortical synapses,  $V_{lin} = \sum g_l K_{ls} E / (1 + g_l K_{li})$ , can be 2 or 3 times larger than the actual somatic potential induced by all excitatory synapses firing in conjunction,  $V_s$  (see rows 5 and 6 in Table 2). For the 10 cortical synapses,  $V_{lin}$  is  $42.1mV$  for  $g_e = 0.005\mu S$ ,  $63.4mV$  for  $g_e = 0.01\mu S$ ,  $85.6mV$  for  $g_e = 0.02\mu S$  and  $109.2mV$  for  $g_e = 0.05\mu S$ . Saturation is less for retinal excitation on the appendages:  $41.6mV$  for  $g_e = 0.005\mu S$ ,  $59.6mV$  for  $g_e = 0.01\mu S$ ,  $76.5mV$  for  $g_e = 0.02\mu S$  and  $92.5mV$  for  $g_e = 0.05\mu S$ .

In summary, we conclude that if  $g_i$  is larger than  $g_e$ , a) inhibition can be very specific, selectively shunting retinal excitation, without b) interfering with electrical activity in the rest of the cell.

During the above analysis, we always assumed that the necks of the dendritic appendages are  $l_N = 1.0\mu m$  long and  $d_N = 0.2\mu m$  thick. However, since Koch and Poggio (1983a) showed that the spine input impedance is a very sensitive function of  $d_N$  and  $l_N$  (essentially

$g_e$	0.005	0.005	0.005	0.01	0.02	0.02	0.02	0.05	0.05
$g_i$	0.005	0.02	0.1	0.1	0.02	0.05	0.2	0.05	0.2
$r, i, c$	25.6	20.5	17.3	23.6	34.2	31.2	28.3	37.7	34.1
	26.4	15.2	6.17	10.0	31.0	21.5	11.0	32.1	18.1
$r, i$	11.1	4.91	1.24	2.37	12.6	7.36	2.39	13.0	5.26
	18.4	9.01	2.46	4.71	24.0	14.4	4.82	25.8	10.6
$c, i$	19.1	17.2	16.4	22.2	28.1	27.4	27.0	32.1	31.8
	15.2	8.10	3.93	5.93	15.5	10.4	6.85	13.8	9.29
$r, c$	31.9	31.9	31.9	37.0	40.6	40.6	40.6	43.5	43.5
	36.5	36.5	36.5	43.1	47.9	47.9	47.9	51.8	51.8
$r$	19.1	19.1	19.1	22.2	24.1	24.1	24.1	25.5	25.5
	28.6	28.6	28.6	36.8	43.4	43.4	43.4	49.1	49.1
$c$	25.1	25.1	25.1	31.4	36.2	36.2	36.2	40.2	40.2

**Table 3.** The somatic depolarization evoked by a 30 synapses for two different spine neck diameters  $d_N$ . The upper set of numbers shows  $V_s$  for  $d_N = 0.1\mu m$ , and the lower for  $d_N = 0.4\mu m$ .  $l_N = 1.0\mu m$  in all cases. For a typical spine (r11 in figure 3), the input resistance increased (decreased) from  $116.77\Omega M$  to  $306.18$  ( $69.05$ ) for  $d_N = 0.1\mu m$  ( $0.4$ ). The transfer resistance to the soma and dendritic input resistances remain unchanged (see table 1). All other parameters are as in table 2.

proportional to  $l_N d_N^{-2}$ ), we will reexamine the validity of some of our results using different neck geometries. Table 3 shows the somatic depolarization evoked by various retinal and cortical inputs for a reduced ( $0.1\mu m$ ) and an enlarged ( $0.4\mu m$ ) spine neck diameter. Comparing these results with table 2, we see that our prior conclusions are robust with respect to the specific details of the spine morphology, emphasizing the dependence of the local veto-operation on the geometry of the spines, i.e. the fact that spines are somewhat removed from the main intracellular pathways.

How do the foregoing results depend on the assumption that inhibition must be of the shunting type, i.e.  $E_i = V_{rest}$ ? Table 4 documents the strength of synaptic interaction for the case  $E_i = -10mV$  (relative to  $V_{rest}$ ); i.e. inhibition reverses at the potassium equilibrium potential. In comparison with the synaptic interaction in the presence of a shunting inhibition, two major conclusions emerge:

(i) Due to the lowered inhibitory reversal potential, the somatic potential  $V_s$  is always lower than for a shunting inhibition. Relative to the inhibitory reversal potential, an hyperpolarizing inhibition is therefore less specific than the shunting inhibition (Koch *et al.* 1982). Thus, for increasingly negative reversal of synaptic potential  $E_i$ , the interaction between excitation and inhibition will become more and more linear, i.e. independent of the spatial location

$g_e$	0.005	0.005	0.005	0.01	0.02	0.02	0.02	0.05	0.05
$g_i$	0.05	0.02	0.1	0.1	0.02	0.05	0.2	0.05	0.2
$r_{i,c}$	24.5	13.8	6.03	-11.7	30.3	22.8	15.1	32.8	22.8
	17.5	9.75	-2.93	0.39	27.5	14.4	-0.37	27.6	7.21
$r_{i,i}$	14.2	3.82	-3.02	-0.96	17.5	8.17	-0.98	18.5	4.31
	10.9	4.84	-4.15	-1.32	23.0	11.0	-1.38	25.3	6.13
$c_{i,i}$	14.0	7.54	4.20	8.44	17.4	14.1	11.9	18.9	16.5
	11.9	1.10	-5.88	-5.14	7.92	-0.42	-6.32	1.94	-5.79
$r_{i,c}$	35.1	35.1	35.1	40.9	44.9	44.9	44.9	47.8	47.8
	37.2	37.2	37.2	44.3	49.8	49.8	49.8	55.2	55.2
$r$	26.0	26.0	26.0	32.4	37.1	37.1	37.1	40.8	40.8
$c$	25.1	25.1	25.1	31.3	36.2	36.2	36.2	40.2	40.2
$i$	-3.25	-4.65	-5.28	-5.28	-4.65	-5.10	-5.37	-5.10	-5.37
	-3.74	-5.85	-7.23	-7.23	-5.85	-6.76	-7.57	-6.76	-7.57

**Table 4.** The somatic depolarization evoked by a 30 synapses. Unlike the preceding tables, the reversal potential of the inhibition is  $-10mV$  relative to  $V_{rest}$ . The seventh row (i), shows the somatic hyperpolarization induced by inhibition alone. All other parameters are as in table 2.

of inhibition with respect to excitation. In other words, for  $E_i \ll V_{rest}$ , inhibition on a spine will reduce the electrical activity throughout the dendrite and will cease acting as a local circuit.

(ii) However, if the specificity of inhibition is judged by the amplitude of the evoked somatic potential  $V_s$  (relative to  $V_{rest}$ ), then a slight hyperpolarizing inhibitory synapse is more specific than a shunting one. For instance, at  $g_e = 0.02\mu S$  and  $g_i = 0.2\mu S$ , conjoint activation of retinal and cortical input will contribute almost nothing to the somatic potential ( $V_s = -0.37$ ) if inhibition is on the dendritic shaft, while about half of the cortical evoked potential still reaches the soma if inhibition is confined to the dendritic appendages ( $V_s = 15.0mV$ ). Activating inhibition in the presence of either cortical or retinal input will almost never result in large hyperpolarizations, except for very strong inhibitory conductance inputs.

In conclusion, inhibition on dendritic appendages, with a slight hyperpolarizing reversal potential, seems like an almost ideal candidate for a) vetoing retinal input without b) neither vetoing cortical input c) nor hyperpolarizing the soma.

## 5.2 Transient Inputs



We will now consider the more realistic situation of time-varying synaptic inputs. Since it is in general impossible to write the depolarization in a closed analytical form, we solve the corresponding Volterra equations (2) and (3) by simple numerical integration. The time course of the excitatory conductance change is given by a generalized alpha function (Jack, Noble and Tsien, 1975)

$$g_e(t) = \text{const} \cdot t^4 e^{-4t/t_{peak}}, \quad (4)$$

and is shown in figure 5a.<sup>1</sup>

For both retinal and cortical evoked excitation, the rise-time ( $t_{peak}$ ) is always set to  $0.5ms$ , resulting in an conductance change lasting about  $1.8ms$ . (compare this with  $\tau_m = 8ms$ ). Since these times are characteristic for the conductance change occurring at a single synapse, they seem to be in general accordance with the intracellularly recorded rise-time of retinal evoked EPSP's of  $1.6 - 3.7ms$  and decay times of  $9.0 - 25ms$  (Eysel, 1976). The time-course of the inhibition,  $g_i(t)$ , is a composite, in order to mimic the relative fast rise-time and the much longer lasting decay time believed to occur at most central synapses (Adams, Constanti and Banks, 1981; Ben-Ari *et al.*, 1981):

$$\begin{aligned} & \text{const}_1 \cdot t^4 e^{-4t/t_{peak}} & \text{if } t < t_{peak} \\ & \text{const}_2 \cdot t^4 e^{-4t/t_{decay}} & \text{if } t > t_{peak} \end{aligned} \quad (5)$$

We usually choose  $t_{peak} = 2.0ms$  and  $t_{decay} = 10ms$ , so that the total inhibitory conductance change lasts about  $32ms$  (see figure 5a). Again, the inhibitory time-course seems to be in broad agreement with the physiologically recorded time course of geniculate IPSP's ( $t_{peak}$  varies between  $2.4 - 4.2ms$  and the duration between  $10 - 50ms$  for those IPSP's most likely to be mediated by the intrageniculate interneuron (Eysel, 1976)). Figure 5b illustrates a typical retinal evoked somatic depolarization with and without the associated shunting inhibition, showing the blockage of the EPSP caused by the second or third retinal spike by inhibition. At higher frequencies more and more current flows through the membrane capacitance and the resulting evoked potentials are smaller than in the steady-state case (about a factor of ten for our parameter values). The nonlinear interaction between synaptic inputs is less strong for the same reason. As a measure of the strength of the vetoing effect of a shunting inhibition, Koch *et al.* (1982) introduced the  $F$ -factor as the ratio of peak somatic depolarization in the absence of inhibition to the depolarization in the presence of inhibition. Koch *et al.* (1983) conjectured that the  $F$ -factor for steady-state inputs ( $F_{dc}$ ), is always larger or equal to the  $F$ -factor when transient inputs are used, independent of the specific time-course assumed. This can be seen quite clearly in figure 6, where  $F$  is

<sup>1</sup>The constant is equal to  $g_{max} t_{peak}^{-4} e^4$ , where  $g_{max}$  is the maximum value of  $g_e(t)$  at  $t = t_{peak}$ .

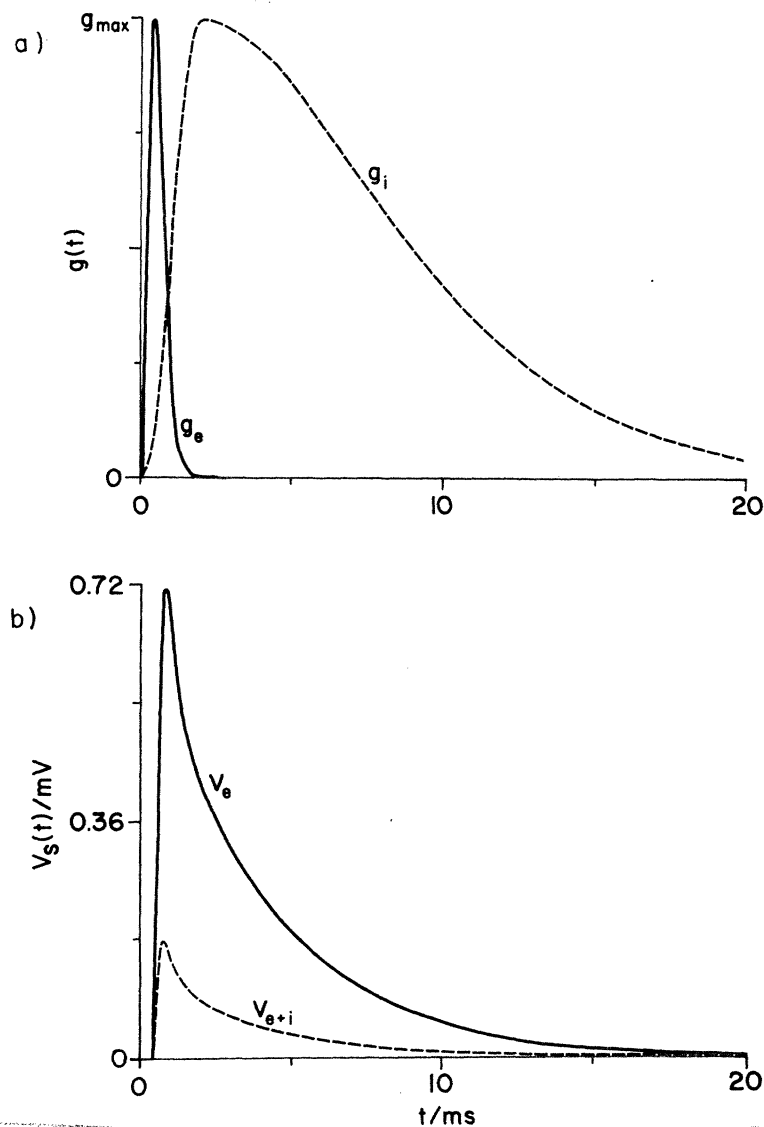


**Figure 5.** (a) The time-course of the excitatory conductance change  $g_e$  with  $t_{peak} = 0.5ms$  and  $g_{max} = 0.01\mu S$  (see eq. (4)). The time-course of inhibition,  $g_i$  is also shown (dashed line) with a rise-time  $t_{peak} = 2ms$ , a decay-time  $t_{decay} = 10ms$  and a peak amplitude  $g_{max} = 0.1\mu S$ . While excitation decays to zero after about  $1.8ms$ , inhibition lasts for about  $32ms$ . (b) The somatic depolarization  $V_s(t)$  in the absence ( $V_e$ ; continuous line) and presence ( $V_{e+i}$ ; dashed line) of a shunting inhibition on a spine at location  $r_{11}$  (figure 2).  $g_i$  is activated  $0.5ms$  prior to the onset of excitation  $g_e$ .  $F$  is given by the peak depolarization without inhibition (0.912) to the maximal depolarization in the presence of inhibition (0.228); i.e.  $F = 4.0$ . A steady-state conductance input  $g_e = 0.01\mu S$  induces a somatic depolarization  $V_s = 6.66mV$  while the shunting inhibition with  $g_i = 0.1\mu S$  reduces  $V_s$  to  $1.01mV$ .

plotted as a function of the relative timing  $\Delta t$  between  $g_e(t)$  and  $g_i(t)$  for a slow and a faster decaying inhibition. Note that  $\Delta t$  is a major determinant of the strength of interaction.

We computed in table 5 the optimal, i.e. the largest,  $F$ -factor as a function of  $\Delta t$  for various locations of excitation and inhibition. One can conclude from these results that while the

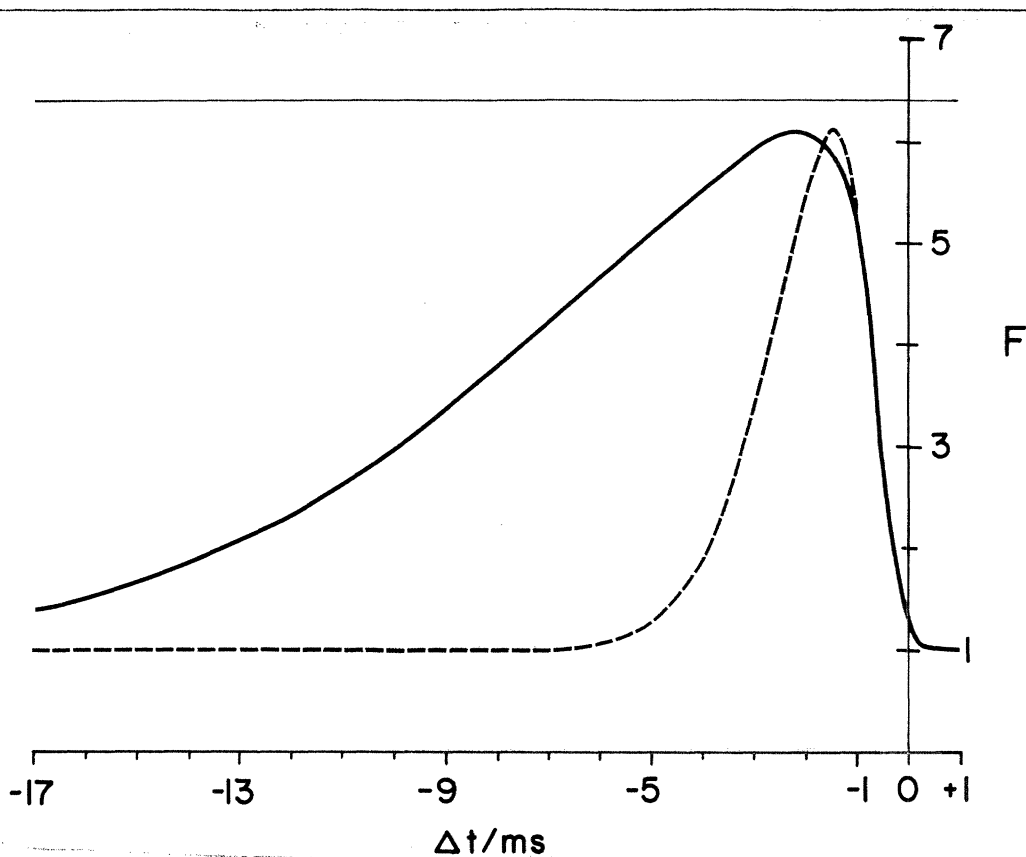


**Figure 6.**  $F$ , the ratio of the peak somatic depolarization without inhibition to the depolarization in the presence of inhibition, as a function of the relative timing  $\Delta t$ , between  $g_e(t)$  and  $g_i(t)$ . Excitation and inhibition are both located on the same appendage ( $r_{11}$  in figure 2). The time-course of both  $g_e(t)$  and  $g_i(t)$  is given in figure 5a (continuous line).  $F$  was also computed for a fast decaying inhibition ( $t_{decay} = t_{peak} = 2.0ms$ ; dashed line). Note that the strength of the nonlinear interaction is always below that for steady-state inputs ( $F_{dc} = 6.39$ ; thin line).

optimal  $F$  is close to  $F_{dc}$  if the locations of excitation and inhibition coincide,  $F$  is 30–50% smaller than  $F_{dc}$  if the locations differ. Therefore, if inhibition is larger than excitation, a long-lasting inhibition on the dendritic appendage vetos very efficiently a shorter-lasting excitation while having little effect on the electrical activity in the rest of the cell.

### 5.3 Underlying Assumption of the Model

How robust are our conclusions with respect to the underlying assumptions, i.e. linearity of the membrane, uniformity of the membrane resistance and the specific values of the cable parameters?

Our basic assumption is that the dendritic membrane is passive, devoid of any regenerative nonlinearities. However, since the recent findings by Jahnsen and Llinas (1984b; see also Llinas and Jahnsen, 1982) of  $Ca^{2+}$ -dependent, high-threshold, dendritic spikes in thalamic

---

e	i	$F_{dc}$	$F$
r11	r11	6.39	6.09
c5	r11	1.53	1.47
r12'	r11	1.20	1.04
r12	r11	1.19	1.04
soma	r11	1.11	1.01

---

**Table 5.**  $F$ , the ratio of peak somatic depolarization in the absence of inhibition to the peak depolarization in the presence of inhibition, for different locations of excitation  $e$  (see figure 2).  $F_{dc}$  is computed under steady-state conditions, while  $F$  is the optimal  $F$  for varying delays  $\Delta t$  between the onset of  $g_e(t)$  and  $g_i(t)$ .  $g_e$  and  $g_i$  are shown in figure 5a.

---

neurons, this assumption may be questionable, although care must be taken in extrapolating from the guinea-pig slice preparation to feline *in vivo* cells. But how would the existence of such all-or-none electrical events in the dendrites affect our conclusions? Two cases must be distinguished. If only the dendrites, but not the appendages, show nonlinear behavior, inhibition in the appendages will still shunt the retinal evoked depolarization. However, how are the dendritic spikes, originating in the periphery, affected if they travel past a spine with activated inhibition? if inhibition is of the shunting type, the situation can be likened to that seen by a spike reaching a bifurcation point, where the axon splits into two daughter branches. Activating the shunting inhibition on the spine is equivalent to increasing the electrical load acting upon the dendritic spike traveling past the spine. As the study by Parnas and Segev showed (1979), propagation failure past the bifurcation point occurs if the combined electrical load of the daughter branches exceeds the load of the main branch by some factor (see also Goldstein and Rall, 1974). Thus, inhibition on the spine would not cause propagation failure, except if the inhibitory conductance change were to be exceptionable large, i.e. the action of inhibition would still be local to the spine. The second possibility is that the appendages themselves might possibly show significant membrane nonlinearities, perhaps initiating the  $Ca^{2+}$  spike.

Since mitochondria are known to take up or release substantial amounts of  $Ca^{2+}$  (Campbell, 1983), this would explain the large number of mitochondria seen in the appendages. Can the shunting inhibition prevent the initialization of the  $Ca^{2+}$  spike? Because the input resistance of the spine is relatively high ( $> 100M\Omega$ ), a small inhibitory conductance change can easily surpass the spine input conductance ( $< 0.01\mu S$ ) in amplitude. Thus, since the dendritic spike requires a high-voltage threshold, activation of even a small inhibitory conductance will prevent large depolarizations (detailed biophysical simulation are in progress). To conclude, even if significant membrane nonlinearities occur in cat geniculate cells, the spine-triad circuit could still implement a very local AND-NOT like gate.

$g_e$	0.005	0.005	0.005	0.01	0.02	0.02	0.02	0.05	0.05
$g_i$	0.005	0.02	0.01	0.1	0.02	0.05	0.2	0.05	0.2
$r_{i,c}$	25.8	16.9	10.4	15.4	31.3	24.9	18.3	33.5	24.9
	26.1	14.0	3.80	6.68	29.6	18.5	6.28	30.1	12.9
$r_{i,i}$	16.2	7.58	1.98	3.79	19.8	11.7	3.85	20.8	6.49
	19.3	9.56	2.69	5.15	25.6	15.6	5.38	28.1	11.9
$c_{i,i}$	16.5	11.4	8.78	12.5	20.0	17.3	15.6	21.4	19.5
	14.8	6.39	1.23	1.88	12.3	5.64	1.11	7.67	1.58
$r_{i,c}$	34.8	34.8	34.8	40.0	43.5	43.5	43.5	46.2	46.2
	36.7	36.7	36.7	43.1	48.2	48.2	48.2	53.4	53.4
$r$	26.3	26.3	26.3	32.4	36.8	36.8	36.8	40.3	40.3
	30.0	30.0	30.0	38.6	45.8	45.8	45.8	52.7	52.7
$c$	25.4	25.4	25.4	31.2	35.4	35.4	35.4	38.9	38.9

**Table 6.** The somatic depolarization evoked by a 30 synapses. The value of the membrane resistance varies across the cell.  $R_m = 800\Omega cm^2$  for the soma and the primary dendrites and  $10020\Omega cm^2$  for the rest of the dendritic tree. The resulting somatic input impedance equals the impedance in the homogeneous case with  $R_m = 4000\Omega cm^2$  (table 1). All other parameters are as in table 2.

A second important assumption is that the neuronal membrane is uniform across the whole dendritic tree. In particular, we assume that both  $C_m$  and  $R_m$  observe the same value throughout the whole cell. In their analysis of cat  $\alpha$ -motoneurons, Fleshman, Segev, Cullheim and Burke (1983) could only match the electrophysiology data with the cellular morphology if they assumed that the membrane resistance increased significantly towards the periphery (as first suggested by Barrett and Crill, 1974). Increasing  $R_m$  with distance, leaving the somatic input resistance unchanged, results in an increase in both input- and transfer-resistance (see table 1). It is surprising, however, how little the resistance values differ for a very different cellular distribution of  $R_m$ . Under these conditions, the nonlinear interaction between synaptic inputs will be slightly enhanced, although the effect is not very strong (see table 6 for an example).

We stress that the quantitative results computed for the HRP-characterized cell depend on the specific values assumed for the cable parameters. By using data collected from a population of geniculate X-cells, we considerably narrow the range of parameter values to be explored. A systematic underestimation of the diameter of the dendrites and especially the dendritic appendages would influence our conclusions, as witnessed by table 3. If the input impedance within the dendritic appendages is little different from that of the dendrites, the *on-the-path* effect would be minimal and the appendages would be unable to perform

the function ascribed to them by us. A similar conclusion applies if either the intracellular resistance or the membrane resistance within spines is very low. In general the larger the difference between the input impedance in the dendritic appendage and in the dendrite just below the appendage, the stronger the *on-the-path* effect; i.e. inhibition on spines reduces the depolarization within the spine very efficiently but does little to inhibit electrical activity outside.

As all our results make abundantly clear, the size of the excitatory and inhibitory conductance changes are critical for the synaptic vetoing mechanism. Precise data about the amplitude and time course of conductance changes at synapses in central neurons is very difficult to obtain. If the change in somatic input resistance is recorded during presynaptic stimulation, values of  $g_i$  well above  $0.1\mu S$  and lasting several hundred milliseconds have been reported in vertebrate central neurons (Ben-Ari *et al.*, 1981; Wunck and Werblin, 1979; Gold and Martin, 1983).

## 6. Discussion

We will argue in this section that the spine-triad circuit is the site of a selective AND-NOT like neuronal gate, limited to the X-system. In section 6.1 we examine the biophysical requirements for our proposed mechanism. Section 6.2 takes a closer look at the neuronal operation implemented by this mechanism and its consequences at the single cell level. In the third and final section, we discuss the circuitry of the LGN and electrophysiological evidence, suggesting that the geniculate interneurons regulate the visual input to the X-system as a function of the behavioral state of the animal.

### 6.1 The Biophysical Mechanism: A Vetoing Operation

The main point of our investigation is reflected in tables 3 and 5. If the inhibition mediated by the interneuron has a reversal potential close to the resting potential of the neuron, it can selectively shunt the retinal evoked depolarization in the spine without affecting the electrical activity outside of this local circuit.

To some extent, however, this analysis represents a worst-case scenario. If more realistic transient conductance changes are considered, the induced postsynaptic potentials are reduced by a factor of 10, due to the losses through the membrane capacitance. As the evoked potential drops, so does the nonlinear interaction between synapses, as documented in figure 7 and table 5. While inhibition becomes only slightly less efficient at reducing the depolarization on the same spine, it influences the potential at other locations far less than the steady-state analysis seems to suggest. Similarly, if the intracellular resistance  $R_i$  in the appendages is larger (perhaps due to the mitochondria) than our assumed value ( $200\Omega cm$ ), our conclusions will be reinforced.

This reasoning points to those conditions for which this behavior will no longer hold true. If the input resistance in the dendritic tree and, especially, in the appendages, is small with respect to the inhibitory conductance change, i.e.  $\tilde{K}_{ii}(0)g_i < 1$ , the synaptic input can be approximated as current and little synaptic interaction occurs (see table 2). A second critical prerequisite for inhibition to effectively reduce the retinal evoked depolarization is that the amplitude of the inhibitory conductance change  $g_i(t)$  is larger than the excitatory one. If  $g_i$  is too small, the interaction between excitation and inhibition is linear, and inhibition will do little to reduce the EPSP.

The third requirement is that the reversal potential of the inhibition is close to the resting potential of the cell. Nonlinear interaction is at its maximum when the inhibition is of the shunting type (Torre and Poggio, 1978; Koch *et al.*, 1982). If the reversal potential associated with inhibition,  $E_i$ , is well below  $E_{rest}$ , excitation and inhibition will interact in an approximately linear way, independent of the geometry of the synaptic arrangement (Koch

*et al.*, 1982). Between these two extremes, however, there is a range of  $E_i$  values for which inhibition will invariably reduce retinal evoked excitation to very low levels while affecting EPSP's from other sources only slightly more than in the shunting case (see table 4).

In this context, the recent findings of Jahnsen and Llinas (1984a,b; see also Llinas and Jahnsen, 1982) warrant a brief discussion. Jahnsen and Llinas, upon recording intracellularly from a large number of *in vitro* guinea-pig thalamic slice neurons, observe two main types of neuronal firing behaviour in all recorded cells. From a membrane potential negative to  $-60mV$ , excitation generated a single burst of high-frequency low-threshold  $Ca^{2+}$ -spikes, followed by approximately  $170ms$  of refractoriness. At membrane potentials positive to  $-55mV$ , activation leads to tonic, repetitive firing. The frequency of this response could always be modulated by the amplitude of the stimulus current (Jahnsen and Llinas, 1984a). McCarley, Benoit and Barrionuevo (1983), when recording in the cat LGN in the dark during waking and sleep, find frequent spike bursts in relay cells during synchronized sleep but almost none in the awake animal. Deschenes, Paradis, Roy and Steriade (1984), recording from the lateral thalamic nuclei in anaesthetized cats, confirmed the results of Jahnsen and Llinas. Their findings suggests that the membrane conductances underlying the burst discharge are located near the soma, as the case in inferior olivary neurons (Llinas and Yarom, 1981). If the reversal potential of inhibition is negative to  $-60mV$ , the dendritic appendage could be the solution adopted by this particular neuronal system to inhibit or "switch" retinal input off without hyperpolarizing the soma or proximal dendrites and thereby eliciting bursts, i.e. thus spines would *isolate*.

To summarize, if inhibition is larger than excitation and has an associated reversal potential close to the resting potential of the cell, then the spine-triad circuit could implement an analog form of a digital AND-NOT gate.

## 6.2 The Neuronal Operation: Inhibiting Retinal Input

We have failed to discuss until now the functional consequences of the vetoing operation for cellular integration. In the most likely picture of events, a burst of spikes from a retinal X-cell leads to a post-synaptic conductance change in both the geniculate X-cell and in the geniculate interneuron. Since there is ample experimental evidence for retinal excitation evoking an monosynaptic EPSP in both projection cells and interneurons (most likely mediated by an excitatory amino acid such as L-aspartate or L-glutamate; Kemp and Sillito, 1982), we assume that the conductance increases, with a reversal potential positive to  $E_{rest}$ . The first spike will thus evoke a depolarization in both the interneuron and the relay cell. If the interneuron is not inhibited itself, the depolarization in the interneuron will trigger within  $0.5 - 1.0ms$  an postsynaptic inhibitory conductance change in the relay cell. There is strong support for the role of GABA as an inhibitory transmitter of the geniculate interneurons



(Sterling and Davis, 1980; Ohara *et al.*, 1983; Sillito and Kemp, 1983; Fitzpatrick, Penny and Schmechel, 1984). Referring to figure 6, we see that activating inhibition after the onset of excitation, for a relatively short-lasting excitation, will not reduce the depolarization by much. However, if inhibition lasts longer than a few milliseconds, the ensuing retinal spikes will be effectively blocked from transmission to the soma. Moreover, the inhibition is expected to be reinforced by every following retinal spike, although Eysel (1976) has shown that repetitive optic tract stimulation reduces the amplitude of the evoked IPSP in the relay cell.

Is there any evidence corroborating our conjecture that the biophysical basis for such an inhibition is a conductance increase with an associated reversal potential close to the resting potential of the cell? McIlwain and Creutzfeldt (1967) explicitly state that suppression of spikes in geniculate cells occurs without any hyperpolarization, although they favor removal of excitation at the retinal level as explanation. Eysel (1976), in an intracellular study, reports an average value of  $-3.35mV$  for the interneuron-mediated hyperpolarization (see also McIlwain and Creutzfeldt, 1967). Moreover, Lindstrom (1982) reports that the IPSP's, associated with an increase in membrane conductance, can easily be reversed by an injection of  $Cl^-$  ions into the cell.<sup>1</sup>

The synaptic veto-operation localized on spines is functionally equivalent to a *presynaptic inhibition*, even if the underlying electrical events occur at a postsynaptic site, since inhibition has little or no influence on the ongoing activity in the rest of the cell (Singer, 1973). We propose that this inhibition is identical with the frequently reported feed-forward inhibition (McIlwain and Creutzfeldt, 1967; Singer, Poppel and Creutzfeldt, 1972; Singer and Bedworth, 1973; Dubin and Cleland, 1977; Lindstrom, 1982). Furthermore, since the spine-triad circuit is limited to X-cells, it follows that geniculate Y-cell's should not show any comparable localized and specific type of inhibition (but see Lindstrom, 1982). Rather, since the inhibitory synaptic profiles are located on the dendritic stems in Y-cells, inhibition will act to reduce the global activity of the cell (Bullier and Norton, 1979).

From what we have said so far, we expect geniculate X-cells to respond in a less sustained way to visual stimuli than retinal X-cells. If the optic tract axon shows a tonic, repetitive firing pattern, the interneuron will be continuously excited and the corresponding dendritic appendage inhibited. Thus, while the first spikes may still elicit sizable EPSP's in the relay cell, all subsequent ones will influence the somatic potential far less than before. The output of the geniculate X-cell is more phasic than its input. This could be likened to a *derivative-like* operation, carried out by the spine-triad circuit.<sup>2</sup> This inhibition is expected

<sup>1</sup>Due to ever-present leakage during intracellular recordings, it is technically very difficult to distinguish a shunting from an hyperpolarizing inhibition. In fact, the very nature of shunting inhibition, i.e. its very local action, makes its detection very difficult.

<sup>2</sup>Richter and Ullman (1982), in a similar proposal, suggested that the retinal dyad performs such a derivative-like operation.

to last until synaptic depletion or habituation inactivates the inhibitory interneuron-relay cell synapse or until the interneuron is inhibited in turn, perhaps indirectly via the feedback loop from the perigeniculate. That geniculate cells are more phasic than their retinal counterparts, is experimentally well known (for instance Cleland, Dubin and Levick, 1971a). Herz *et al.* (1964) measured the mean interspike distributions from optic tract recordings (12–20ms), while the most frequent intervals in geniculate neurons have a duration between 35–70ms (see also Singer, Poppel and Creutzfeldt, 1972). In a similar vein, So and Shapley (1979) conclude that a stimulus which produces a very sustained response at the retinal level may produce a very transient response at the geniculate level. However, given the complex geniculate morphology and synaptology, we do not believe that the sole function of the spine-triad circuit is to perform a derivative-like operation on the retinal X-input.

### 6.3 The Function: Selectively Gating Visual Input to the X-System

Based on our analysis, what is the function of the spine-triad circuit? Any explanation must account for the three distinct elements making up the spine-triad circuit: (i) the dendritic appendage, (ii) the synapse from the retinal afferent onto the interneuron and (iii) the synapse from the interneuron onto the relay cell.

#### 6.3.1 Spines isolate:

Our simulation of the biophysical properties of the relay cell show that spines act as local circuit, isolating the electrical activity in the soma and in the dendrites from electrical events inside the spine. The spine-triad arrangement can be considered as analog implementation of a logical AND-NOT gate (Koch and Poggio, 1983a,b). The retinal input can be selectively switched off without inhibiting ongoing activity in the rest of the cell, as suggested already by Hamori *et al.* (1974). The local nature of the inhibition will even be retained if dendritic spikes occur under physiological conditions, since the major reason for the isolation effect resides in the particular geometry of the spine.

#### 6.3.2 Inhibition depends on the activity in the retinal afferent:

But under what conditions will inhibition be activated? Because the input impedance of the thin and slender dendrites of the interneurons is expected to be quite high, the retinal input associated with the triad will most likely evoke a large EPSP in the dendrite of the interneuron. However, if this EPSP fails to evoke regenerative nonlinearities in the membrane of the interneuron, the influence of the EPSP at the soma or at other sites will be slight, given the small nature of the processes and the correspondingly high attenuation. Each process of the interneuron (see figure 1) may essentially act as a "subunit" of its own, integrating electrical activity independent of activity in adjacent "subunits" (Ralston, 1971). In other words, the function of the triadic synaptic relationship would be to faithfully inhibit

the retinal evoked excitation in the relay cell at a single site. The integrating ability of the cell change may change dramatically if the retinal excitation triggers (dendritic) spikes in the interneuron, such as high-threshold  $Ca^{2+}$  spikes. These spikes could propagate to the soma and into other dendritic branches. A similar situation is known to occur in amacrine cells of the vertebrate retina, which have no clearly defined axon and show both graded potentials and spikes in the dendritic tree (Miller, 1979). If the spike invades the presynaptic processes without significant attenuation, it will activate the dendro-dendritic synapses, blocking retinal input at all sites postsynaptic to the interneuron. If the interneuron is presynaptic to several relay cells, the electrical activity in these cells will be reduced within a few milliseconds. Interestingly, Wong (1970) reports in the squirrel monkey dendro-dendritic synapses from the soma of a presumed interneuron onto the dendrite of a relay cell. Thus, the interneuron could inhibit adjacent X-cells directly at the dendritic stems or even at the soma, reducing their global activity. If these adjacent X-cells have neighboring or partially overlapping receptive fields, this mechanism could account for the strong peripheral antagonism seen in LGN cells (Hubel and Wiesel, 1961; Fukuda and Stone, 1976). Retinal X-cells respond better than geniculate X-cells to uniform illumination of their receptive fields. This effect is particularly clear in measurements of spatial contrast sensitivity (Derrington and Fuchs, 1979), which show a sharper loss of sensitivity in X- than in Y-cells as the spatial frequency falls below the optimum; curves obtained from geniculate Y-cells are not unlike those obtained from Y-cells in the retina (Lennie, 1980).

The geniculate interneurons are in all likelihood also responsible for the "reciprocal lateral inhibition" seen between "on"- and "off"-geniculate relay cells (Singer and Creutzfeldt, 1970): the powerful "on"-inhibitory effects elicited from the center of an "off"-center cell could be driven by the interneuron-mediated activity from an "on"-center optical tract axon and indeed the latency of the IPSP's involved in this type of response support this view. Equally, a component of the center antagonistic inhibitory input to an "off"-center cell could involve a short latency inhibitory input derived from an "on"-center optical tract axon (Sillito and Kemp, 1983).

As we mentioned above, one effect of our proposed veto-operation is to increase the transiency of the retinal input, limiting at the same time the maximal firing frequency of the geniculate cell. For increasing firing frequency in the optic tract axon, the inhibition at the spine will be continuously active, preventing any retinal input from contributing to the somatic potential. We therefore expect the onset of saturation with increasing stimulus contrast to occur earlier in geniculate than in retinal X-cells (see figure 7 in Maffei and Fiorentini, 1973). From the time-course of inhibition, one can approximately predict for what firing frequencies of the retinal afferent saturation is expected to occur. If inhibition peaks at  $2ms$  and decays with a time-constant of  $10ms$ , the retinal input is blocked for about  $20ms$  following the first spike (see figure 6). For such a synaptic time-course, the relay

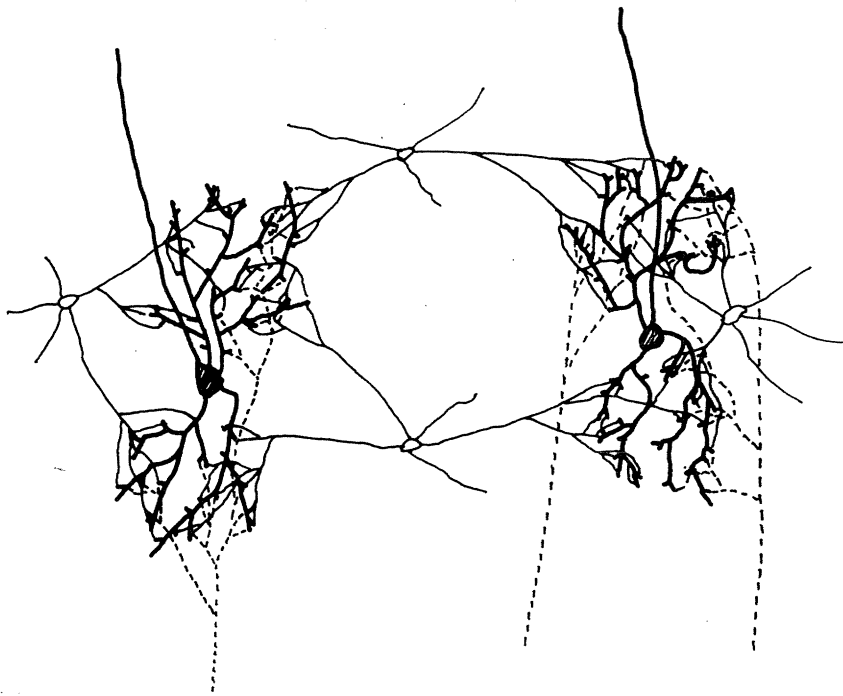


**Figure 7.** Schematic drawing illustrating the possible relationship between geniculate X-relay cells (heavy lines), geniculate interneurons (without projecting axon; light lines) and optic tract fibers (dashed lines). There are about two X-relay cell for every interneuron. Little is known about the global relationship between interneurons and projection cells. We show one likely possibility, where several interneurons control the visual input of one X-relay cell and one to three optic tract axons converge onto a single X-relay cell.

cell is expected to faithfully follow the input frequency up to about  $50\text{Hz}$ , subsequently showing no further increase in firing frequency. Such contrast-dependent inhibition has been uncovered by Berardi and Morrone (1984) during the iontophoretic application of bicuculline, an antagonist of GABA, to geniculate X- and Y-cells. Recording the mean spike activity as a function of the contrast of the visual stimulus, they report that the drastic reduction in inhibition upon application of bicuculline is independent of stimulus contrast for Y-cells but increases for increasing stimulus contrast, i.e. increasing optic tract activity, in X-cells. Bullier and Norton (1979) stress as major difference between retinal and geniculate X- and Y-cells their differing spontaneous and driven electrical activities, geniculate X-cells firing far less than retinal X-cells. Geniculate Y-cells, on the other hand, show only a small decrease in spontaneous and driven activity in comparison with Y ganglion cells (see also Fukuda and Stone, 1976).

In summary, the most likely function of the synapse connecting the retinal afferent with the interneuron is a) contrast dependent enhancement of the center-surround organization and "reciprocal lateral inhibition" and b) a reduction in the total amount of retinal excitation.

### 6.3.3 The interneuron controls the visual input to geniculate X-cells:

The major point emerging from our analysis is that the degree of retinal excitation of

geniculate X-cells can be controlled by the geniculate interneuron. If the presynaptic process is inhibited, retinal excitation will fail to activate the inhibitory interneuron-relay cell synapse, and the X-cell will be *disinhibited*. Depending on the cable properties of the interneuron, inhibition could be local to one presynaptic process or global to the whole cell. How much of the retinal input to a single X-cell is controlled by a single interneuron cannot be determined without reliable anatomical data on the degree of convergence in the LGN and the total number of interneurons (see figure 7).

The interneuron seems like an ideal locus for such a gating function due to its potential ability to process information from a wide variety of sources. Apart from the well-documented retinal input, it is also postsynaptic to nucleus reticularis, corticofugal and midbrain fibers (see figure 8):

**Input from the retina:** We will not review here the evidence showing that physiologically characterized X-optic tract axons converge onto the interneuron (see section 2). A very intriguing finding, without anatomical confirmation, concerns the possible convergence of Y-optic tract axon onto interneurons. Singer and Bedworth (1973) discuss the electrophysiological evidence suggesting a short-delay, inhibitory pathway between geniculate Y- and X-cells (for more evidence see Hoffmann, Stone and Sherman, 1972; Noda, 1975a; Dubin and Cleland, 1977). The mixing of X- and Y-signals in the interneuron could be mediated by either a direct projection from the Y-optic tract axon onto the interneuron or via the intrageniculate axon collaterals of the geniculate Y-relay cell (Friedlander *et al.*, 1981).

**Input from the thalamic reticular nucleus:** The thalamic reticular nucleus (TRN) is a sheet-like structure enveloping much of the dorsal thalamus and receiving a strong projection from the visual cortex and the midbrain reticular formation cortex (Schmielau, 1979). Moreover, the perigeniculate nucleus, a substructure of the TRN mediating visual input (Ahlsen, Lindstrom and Lo, 1982b), receives collaterals from geniculate X- and Y-relay cells (Dubin and Cleland, 1977; Ahlsen, Lindstrom and Sybirska, 1978; Friedlander *et al.*, 1981; Ahlsen and Lindstrom, 1982). This pathway mediates the recurrent inhibition seen in geniculate relay cells. Most, if not all, of the neurons in the TRN appear to be GABAergic and thus almost certainly inhibitory (Ohara *et al.*, 1983; Oertel *et al.*, 1983; Fitzpatrick *et al.*, 1984). The arrangement of the efferent connections from the TRN onto the LGN is topographical (Minderhoud, 1971). The ultrastructural basis for this projection are the F1 symmetric synapses (Ohara *et al.*, 1980), presynaptic to the geniculate interneuron and to the Y-relay cell (Guillery, 1969a; Famiglietti and Peters, 1972; Wilson *et al.*, 1984; Hamos *et al.*, 1984b). Ahlsen,

Lindstrom and Lo (1982a) report that activation of the perigeniculate interneurons causes a marked depression of the feed-forward inhibition mediated by the geniculate interneuron.

**Input from the midbrain:** Electrophysiology indicates that the LGN receives input from the brainstem, including the midbrain reticular formation (MRF; for a recent anatomical survey consult Hughes and Mullikin, 1984). It has been suggested in particular that brain-stem neurons have a long-latency (30 – 40ms), long-lasting (> 100ms) disinhibitory effect on relay cells (Fukuda and Iwama, 1971; Singer, 1973). Ahlsen, Lindstrom and Lo (1984) showed that the underlying mechanism is an inhibition, lasting about 100ms, of both perigeniculate and geniculate interneurons. Likewise, norepinephrine-containing neurons of the locus coeruleus have been shown to inhibit the interneuron (Nakai and Takaori, 1974). Of particular interest to us are two studies reporting a differential effect of midbrain stimulation on geniculate X- and Y-cells. Using area/threshold measurement to assess peripheral antagonism, Fukuda and Stone (1976) showed that the effect of MRF stimulation is to reduce the surround inhibition in X-cells, while leaving the surround in Y-cells virtually unchanged. Foote *et al.* (1977) find that the response of X-cells to optic chiasm stimulation is enhanced when preceded by a conditioning pulse to the midbrain but depressed in Y-cells. This finding, together with the report of Ahlsen *et al.* (1984; see also Ahlsen and Lo, 1982), lends strong support to our hypothesis that the specific shunting of retinal input is limited to X-cells.

**Input from the visual cortex:** It has been demonstrated in a large number of anatomical studies that the LGN receives a prominent topographic projection from the visual cortex, originating in layer 6 pyramidal cells (Jones and Powell, 1969b; Gilbert and Kelly, 1975; Tsumoto, Creutzfeldt and Legendy, 1978; for a summary see Macchi and Rinvik, 1976). The ultrastructural basis for this projection are the RSD asymmetric synapses, found in large numbers on X- and Y-relay cells and on the interneuron (Guillery, 1969a,b; Jones and Powell, 1969b; Wilson *et al.*, 1984; Hamos *et al.*, 1984). The presynaptic fibers are among the thinnest myelinated fibers in the LGN, implying correspondingly low conduction velocities and large delays. Cortical stimulation excites both geniculate interneurons and relay cells monosynaptically, with a latency between 2.8 and 4.5ms (Dubin and Cleland, 1977; Ahlsen, Grant and Lindstrom, 1982).

Since geniculate interneurons seem to receive excitatory and inhibitory projections from a host of cortical, thalamic and brain stem systems, we suggest that they control the flow of visual information into the X-system. The postsynaptic effect of the corticofugal projection is

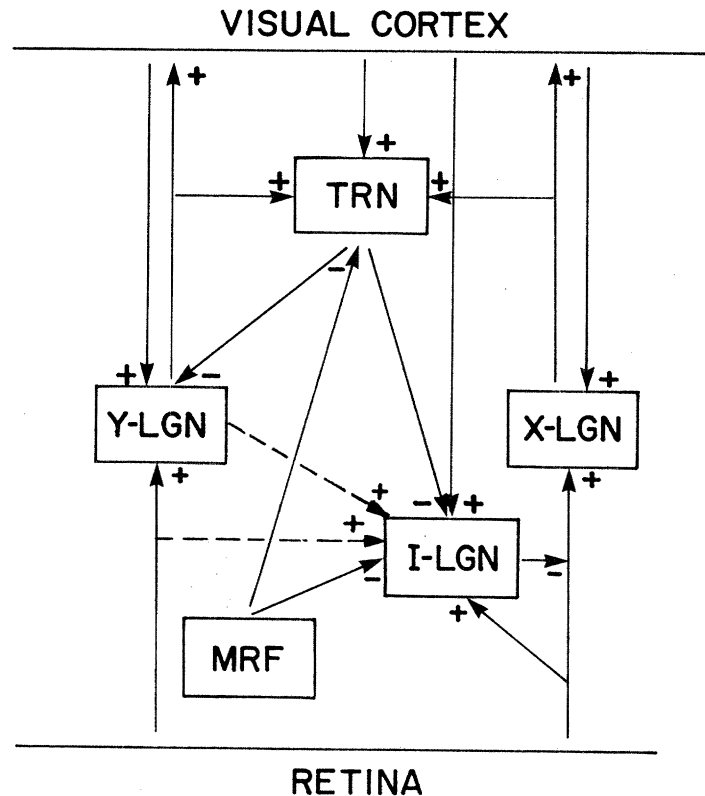


**Figure 8.** Schematic diagram illustrating the functional relationships between the LGN and its main afferent and efferent pathways. MRF stands for the midbrain reticular formation, TRN for the reticular formation of the thalamus and I-LGN for the geniculate interneuron. These interneurons control the visual input to the X-system via the spine-triad circuit, which is functionally equivalent to presynaptic inhibition. Physiological evidence indicates a possible separate Y-input to the geniculate interneurons. The sign next to each arrow indicates the probable action on postsynaptic potential. Note that, following Jahnsen and Llinas (1984a) and Crick (1984), the net action of an inhibitory input to LGN cells might be the initiation of a short burst of spikes.

to reduce retinal input, while simultaneously depolarizing the cell. In other words, the X-cell will be decoupled from its input while being excited (perhaps "mimicking" visual input). The ascending brain stem pathway could mediate a long-lasting disinhibition of relay cells as a function of the global behavioral state of the animal, e.g. sleep, paradoxical sleep, drowsiness and arousal, while the excitatory action of the Y-system onto the interneuron could be responsible for saccadic suppression and other motion-dependent effects in the X-system. We will briefly discuss the possible involvement of this circuitry in visual attention and saccadic suppression.

#### 6.3.4 Selective attention: Varying the extent of the receptive field of X-cells

If geniculate X-cells receive excitatory input from only a few retinal X-cells with overlapping but shifted receptive fields (Cleland, Dubin and Levick, 1971b; Levick, Cleland and Dubin,

1972; Singer and Bedworth, 1973), activating the appropriate interneuron could selectively "disconnect" the relay cell from its retinal input, i.e. the receptive field of the geniculate cell is reduced in size and extent. Since visual acuity is presumably related to receptive field size, reducing their extent should lead to an increase in the ability of the system to localize and resolve fine details in the visual scene. Because of the relatively small extent of the interneuron ( $\approx 100 - 200\mu m$ ), the change in receptive field size can be limited to one or very few X-cells, i.e. to a very small portion of the visual field. If the visual system wants to attend to some location, i.e. resolve some area in visual space in great detail, the corresponding interneurons are excited, for instance by the excitatory corticofugal projection. This reduces the retinal evoked EPSP's in the X-relay cell postsynaptic to the interneuron, without inhibiting the EPSP's generated at other sites in the relay cell. Note that the local nature of inhibition is the crucial element of this mechanism.

In a study of the effect of somatic stimulation, i.e. stroking and caressing, upon cat geniculate relay cells, Godfraind and Meulders (1969; Meulders and Godfraind, 1969) report that in both the anesthetized and the alert cat, the receptive field of geniculate cells is enlarged when preceded by a somatic stimulation. Moreover, LGN cells discharge to a light stimulus applied outside the border of the receptive field as determined without any somatic stimulation. We believe that this effect is mediated by an excitatory action of the somatic stimulation on midbrain neurons. These inhibit in turn the geniculate interneuron, removing the shunting inhibition in the relay cells and enabling all retinal input to contribute to the receptive field.

### 6.3.5 Selective attention: Controlling the strength of visual input to X-cells

One prominent behavior influencing geniculate activity is sleep and arousal (Singer, 1977). Coenen and Vendrik (1972) showed that the amplitude of visual evoked EPSP's in *non-anaesthetized*, paralyzed cats is smaller during sleep than during wakefulness. The smallest values were recorded if a light anaesthesia was used. Equally, Livingstone and Hubel (1981) report increased spontaneous firing rates and enhanced responses to optimal stimuli upon arousal (see also McCarley *et al.*, 1983). As a number of studies have suggested that two monoaminergic brain-stem regions, the raphe nuclei and the locus coeruleus, fire more rapidly during periods of increased alertness such as paradoxical sleep and arousal (Chu and Bloom, 1973; Foote, Aston-Jones and Bloom, 1980), we propose that they influence retino-cortical transmission by selectively inhibiting geniculate interneurons. This hypothesis is in accordance with the evidence by Ahlsen *et al.* (1984) of a long-lasting IPSP ( $\approx 100ms$ ) in interneurons upon stimulation of the MRF. During arousal, when increased alertness is required, the brain-stem inhibits the interneuron thereby disinhibiting the corresponding X-relay cells.

Of potential great interest is the possible involvement of the LGN in selecting and detecting



interesting or conspicuous features in the visual scene as proposed by a number of studies (Yingling and Skinner, 1977; Crick, 1984; Koch and Ullman, 1984). Crick conjectures that the TRN hyperpolarizes in a very specific manner the projection cells in the LGN, thereby de-inactivating the  $Ca^{2+}$ -current found by Jahnsen and Llinas (1984a,b), leading to the burst behavior. Since the X-relay cells seem to receive few synapses arising in the TRN, this mechanism would be limited to Y-relay cells. Alternatively, we would like to suggest that *selective visual attention* could act upon the geniculate interneurons, suppressing undesired or uninteresting visual information. Such a role of the geniculate X-system is suggested by the experiments of Posner, Cohen and Rafal (1982). They report in human subjects a long-lasting (up to 400ms) inhibition of the processing efficiency of a cued location, once attention has been withdrawn.

One cautionary note. Most attention related phenomena in the visual cortex can only be observed electrophysiologically in the awake, behaving preparation (see for instance Bushnell, Goldberg and Robinson, 1981). Since the overwhelming majority of studies of the LGN have employed anaesthetized and/or paralyzed animals, it is not surprising that little evidence for attention-dependent transmission exists.

#### **6.3.6 Saccadic suppression: Controlling the strength of visual input to X-cells**

The threshold for visual perception rises abruptly with fast eye movements, explaining why the external world is stable and does not blur during saccades (Helmholtz, 1866). Typically, the luminance threshold for flashes rises by about a factor of three during saccades (Riggs, Merton and Morton, 1974; Brooks and Fuchs, 1975). Furthermore, the neural mechanisms sensitive to movement are damped during saccades, thereby preventing perception of image motion (Burr, Holt, Johnstone, Ross, 1982). The latter phenomena most likely requires efferent feedback (Burr *et al.*, 1982; Riggs *et al.*, 1974). Saccadic suppression does seem to be, however, also a partly visual mediated phenomena: moving a visual stimulus at saccadic speeds yields the same threshold changes as moving the eyes (MacKay, 1970; Brooks and Fuchs, 1975).

One neurophysiological correlate of saccadic suppression is an impaired transmission of visual information through the LGN during fast movements. During saccadic eye movements or during fast stimulus movements, geniculate Y-cells respond with a burst discharge while the discharge of X-cells is completely suppressed (Noda, 1975a,b). The time-course of this depression is similar to that of the Y-cell burst discharge. The changes in firing pattern are caused by afferent impulses arising in the retina, since they disappeared completely in total darkness. Similarly, Singer and Bedworth (1973) report that X-cells are effectively inhibited when Y-cells are activated by fast moving contrasts ( $> 200^\circ/sec$ ), indicating that the depression of X-cells is a consequence of retinal processes initiated by the image movement during a saccades and does not depend on eye movement *per se*. It seems

therefore likely, that the elevation of threshold seen during saccadic suppression is at least partially due to the inhibitory pathway from the geniculate Y-system on the geniculate X-system, mediated by an excitatory Y-input to the interneurons.<sup>3</sup>

The disinhibitory discharge observed by Singer and Bedworth (1974) starting some 40–60ms before the end of a saccade, which could also be elicited by MRF stimulation, would then act selectively on geniculate X-cells, terminating the effects of saccadic suppression and restoring the excitability of X-cells. This conclusion is reinforced by a study of the relationship between the frontal eye field (FEF) and the LGN (Tsumoto and Suzuki, 1976). Upon electrical stimulation of the FEF, more than a third of the geniculate relay cells increased their response probabilities to optic tract stimuli for 100–400ms following the stimulus. These cells were classified as X-cells. Of the 4 geniculate non-relay cell recorded, three showed clear signs of inhibition, while one was excited by FEF stimulation. Judging from the temporal relationship between saccadic induced inhibition and FEF facilitation, Tsumoto and Suzuki conclude that FEF begins to exert its facilitatory effect on geniculate X-cells about 50–100ms after saccadic suppression.

#### 6.4 Why Is the Spine-Triad Circuit Limited to the X-System?

Finally, we have to address the most crucial question of this study. Why is the spine-triad circuit essentially limited to the X-system? Or, why should the action of inhibition on geniculate Y-cells be global, while inhibition on geniculate X-cells is very localized and selective? We will give an overview of the main difference between the X- and the Y-system at the level of the LGN, before both pathways enter the visual cortex (for an overview see Lennie, 1980 and Sherman and Spear, 1982; for specific details consult Cleland *et al.*, 1971; Hoffmann *et al.*, 1972; Derrington and Fuchs, 1979; Bullier and Norton, 1979; So and Shapley, 1979; Frishman, Schweitzer-Tong and Goldstein, 1983). Originally, X and Y cells were classified according to their linear or non-linear spatial summation behavior (Enroth-Cugell and Robson, 1966; Shapley and Hochstein, 1975). Moreover, in the LGN, as in the retina, Y-relay cells are more sensitive to fast moving contrasts such as bars and gratings, have larger receptive fields (the diameter of the central region ranges between 1° and 4°) than X-cells (between 0.5° and 1.5°) and thus better spatial resolution than X-cells. Y-cells also respond better than X-cells to low spatial frequencies, i.e. to uniform illumination of the receptive field, whereas X-cells are more sensitive to changes in position and spatial phase. An important factor in the reduced sensitivity of X-cells for low spatial frequencies is their strong surround. Almost all Y-cells exhibit the so-called "shift-effect", i.e. a response to a sudden displacement of a peripheral stimulus well outside their conventional

---

<sup>3</sup>A further function of the inhibitory influence of the Y-system onto the X-system, mediating backward visual pattern masking, was suggested by Breitmeyer and Ganz (1976).

receptive field, but very few X-cells do. Y cells tend to give more transient responses to standing contrast than X-cells, although this distinction is not clear-cut. Lastly, Y-cells in the LGN have faster-conducting axons than X-cells. These diverse properties of X and Y cells suggest that they have different tasks to perform. Thus, the chief role of Y cells may be to provide basic form analysis and to alert the cortex to fast moving objects, while the X-system is responsible for the high-resolution analysis of the visual scene, or parts of it. In fact, Sherman has postulated on the basis of behavioral experiments done on normal, dectriate and visually deprived cats, that the Y-cell pathway is responsible for the analysis of basic forms while the X-cell pathway adds detail and raises spatial resolution and position sensitivity (Sherman, 1982 and 1984).

Our analysis suggests that activity in the Y-pathway travels relatively unaffected through the LGN, while transmission through the X-pathway can be modified considerably. One could speculate that the perception mediated by the Y-system is crucial to the survival of the animal and must always remain undisturbed. It provides the animal with a basic, large-scale visual map of his environment. Attending to some interesting cue in the visual scene requires, however, a very sensitive and high-resolution system. The X-system, by adapting to the nature of the stimulus and the behavioral state of the animal, can provide such detail.

**Acknowledgment:** I am deeply indebted to Murray Sherman and his group, for discussing all of his results with me, his many suggestions and for never being tired of my phone calls. Stewart Bloomfield provided the HRP material and the electrophysiological data upon which the computer analysis is based. Jim Hamos introduced me to the ultrastructure of the geniculate circuitry. Thanks to Mike Friedlander, John Maunsell, Tom Collett and Andrew Parker for critically reading the manuscript. Tomaso Poggio made it all possible. The author is supported by the Fritz Thyssen Stiftung.

## References

- Adams, P.R., Constanti, A. and Banks, F.W., "Voltage clamp analysis of inhibitory synaptic action in crayfish stretch receptor neurons", *Fed. Proc.*, **40**, 2637-2641, 1981.
- Ahlsen, G., Grant, K. and Lindstrom, S., "Monosynaptic excitation of principal cells in the lateral geniculate nucleus by corticofugal fibers", *Brain Res.*, **234**, 454-458, 1982.
- Ahlsen, G. and Lindstrom, S., "Excitation of perigeniculate neurones via axon collaterals of principal cells", *Brain Res.*, **236**, 477-481, 1982.
- Ahlsen, G., Lindstrom, S. and Lo, F.-S., "Interactions between inhibitory interneurons in lateral geniculate nucleus of the cat", *J. Physiol.*, **NNN**, 38P-39P, 1982a.
- Ahlsen, G., Lindstrom, S. and Lo, F.-S., "Functional distinction of perigeniculate and thalamic reticular neurons in the cat", *Exp. Brain Res.*, **46**, 118-126, 1982b.
- Ahlsen, G., Lindstrom, S. and Lo, F.-S., "Inhibition from the brain stem of inhibitory interneurons of the cat's dorsal lateral geniculate nucleus", *J. Physiol.*, **347**, 593-609, 1984.
- Ahlsen, G. and Lo, F.-S., "Projection of brain stem neurons to the perigeniculate nucleus and the lateral geniculate nucleus in the cat", *Brain Res.*, **238**, 433-438, 1982.
- Barrett, J.N., "Motoneuron dendrites: role in synaptic integration", *Fed. Proc.*, **34**, 1398-1407, 1975.
- Barrett, J.N. and Crill, W.E., "Specific membrane properties of cat motoneurons", *J. Physiol. Lond.*, **239**, 301-324, 1974.
- Ben-Ari, Y., Krnjevic, K., Reiffenstein, R.J. and Reinhardt, W. "Inhibitory conductance changes and action of  $\gamma$ -aminobutyrate in rat hippocampus", *Neurosci.*, **6**, 2445-2463, 1981.
- Berardi, N. and Morrone, M.C., "Gabergic inhibition of X- and Y-cells in cat LGN", In preparation, 1984.
- Bloomfield, S. and Sherman, M.S., "Morphometric and electrical properties of neurons in the lateral geniculate nucleus of the cat", *Neurosci. Abst.*, **10**, 1984.
- Boycott, B.B. and Wässle, H., "The morphological types of ganglion cells of the domestic cat's retina", *J. Physiol.*, **240**, 397-419, 1974.
- Breitmeyer, B.G. and Ganz, L., "Implications of sustained and transient channels for theories of visual pattern masking, saccadic suppression, and information processing", *Psychol. Rev.*, **83**, 1-36, 1976.
- Brooks, B.A. and Fuchs, A.F., "Influence of stimulus parameters on visual sensitivity during saccadic eye movement", *Vision Res.*, **15**, 1389-1398, 1975.

- Brown, T.H., Perkel, D.H., Norris, J.C. and Peacock, J.H., "Electronic structure and specific membrane properties of mouse dorsal root ganglion neurons", *J. Neurophysiol.*, **45**, 1-15, 1981.
- Bullier, J. and Norton, T.T., "Comparison of receptive-field properties of X and Y ganglion cells with X and Y lateral geniculate cells in the cat", *J. Neurophysiol.*, **42**, 274-291, 1979.
- Burr, D.C., Holt, J., Johnstone, J.R. and Ross, J., "Selective depression of motion sensitivity during saccades", *J. Physiol.*, **333**, 1-15, 1982.
- Bushnell, M.C., Goldberg, M.E. and Robinson, D.L., "Behavioral enhancement of visual responses in monkey cerebral cortex. I. Modulation in posterior parietal cortex related to selective visual attention", *J. Neurophysiol.*, **46**, 755-772, 1981.
- Butz, E.G. and Cowan, J.D., "Transient potentials in dendritic systems of arbitrary geometry", *Biophys J.*, **14**, 661-680, 1974.
- Campbell, A.K., *Intracellular calcium. Its universal role as regulator*, John Wiley, New York, 1983.
- Chu, N.-S. and Bloom, F.E., "Norepinephrine-containing neurons: changes in spontaneous discharge patterns during sleeping and waking", *Science*, **179**, 908-910, 1973.
- Cleland, B.G., Dubin, M.W. and Levick, W.R., "Sustained and transient neurones in the cat's retina and lateral geniculate nucleus", *J. Physiol.*, **217**, 473-496, 1971a.
- Cleland, B.G., Dubin, M.W. and Levick, W.R., "Simultaneous recording of input and output of lateral geniculate neurones", *Nature New Biol.*, **231**, 191-192, 1971b.
- Coenen, A.M.I. and Vendrik, A.J.H., "Determination of the transfer ratio of cat's geniculate neurons through quasi-intracellular recordings and the relation with the level of alertness", *Exp. Brain Res.*, **14**, 227-242, 1972.
- Crick, F., "The function of the thalamic reticular complex: the searchlight hypothesis", *Proc. Natl. Acad. Sci. USA*, In the press, 1984.
- Derrington, A.M. and Fuchs, A.F., "Spatial and temporal properties of X and Y cells in the cat lateral geniculate nucleus", *J. Physiol.*, **293**, 347-364, 1979.
- Deschenes, M., Paradis, M., Roy, J.P. and Steriade, M., "Electrophysiology of neurons of lateral thalamic nuclei in cat: resting properties and burst discharges", *J. Neurophysiol.*, **51**, 1196-1219, 1984.
- Dubin, M.W. and Cleland, B.G., "Organization of visual inputs to interneurons of lateral geniculate nucleus of the cat", *J. Neurophysiol.*, **40**, 410-427, 1977.

Eysel, U.Th., "Quantitative studies of intracellular postsynaptic potentials in the lateral geniculate nucleus of the cat with respect to optic tract stimulus response latencies", *Exp. Brain Res.*, **25**, 469-486, 1976.

Famiglietti, E.V., "Dendro-dendritic synapses in the lateral geniculate nucleus of the cat", *Brain Res.*, **20**, 181-191, 1970.

Famiglietti, E.V. and Peters, A., "The synaptic glomerulus and the intrinsic neuron in the dorsal lateral geniculate nucleus of the cat", *J. comp. Neurol.*, **144**, 285-334, 1972.

Fitzpatrick, D., Penny, G.R. and Schmechel, D.E., "Glutamic acid decarboxylase-immunoreactive neurons and terminals in the lateral geniculate nucleus of the cat", *J. Neurosci.*, **4**, 1809-1819, 1984.

Fleshman, J.W., Segev, I., Cullheim, S. and Burke, R.E., "Matching electrophysiological with morphological measurements in cat  $\alpha$ -motoneurons", *Neurosci. Abst.*, **9**, 102.19, 1983.

Foote, S.L., Aston-Jones, G. and Bloom, F.E., "Impulse activity of locus coeruleus neurons in awake rats and monkeys is a function of sensory stimulation and arousal", *Proc. Natl. Acad. Sci. USA*, **77**, 3033-3037, 1980.

Foote, W.E., Mordes, J.P., Colby, C.L. and Harrison, T.A., "Differential effect of midbrain stimulation on X-sustained and Y-transient neurons in the lateral geniculate nucleus of the cat", *Brain Res.*, **127**, 153-158, 1977.

Friedlander, M.J., Lin, C.-S., Stanford, L.R. and Sherman, S.M., "Morphology of functionally identified neurons in lateral geniculate nucleus of the cat", *J. Neurophysiol.*, **46**, 80-129, 1981.

Friedlander, M.J., Lin, C.-S. and Sherman, S.M., "Structure of physiologically identified X- and Y-cells in the cat's lateral geniculate nucleus", *Science*, **204**, 1114-1117, 1979.

Friedlander, M.J. and Stanford, L.R., "Effects of monocular deprivation on the distribution of cell types in the LGN<sub>d</sub>: A sampling study with fine-tipped micropipettes", *Exp. Brain Res.*, **53**, 451-461, 1984.

Frishman, L.J., Schweitzer-Tong, D.E. and Goldstein, E.B., "Velocity tuning in cells in dorsal lateral geniculate nucleus and retina of the cat", *J. Neurophysiol.*, **50**, 1393-1414, 1983.

Fukuda, Y. and Iwama, K., "Reticular inhibition of internuncial cells in the rat lateral geniculate body", *Brain Res.*, **35**, 107-118, 1971.

Fukuda, Y. and Stone, J., "Evidence of differential inhibitory influences on X- and Y-type relay cells in the cat's lateral geniculate nucleus", *Brain Res.*, **113**, 188-196, 1976.

Gage, P.W. and McBurney, R.N., "Miniature end-plate currents and potentials generated by quanta of acetylcholine in glycerol-treated toad satorius fibers", *J. Physiol.*, **226**, 79-94, 1972.

Gilbert, C.D. and Kelly, J.P., "The projections of cells in different layers of the cat's visual cortex", *J. Comp. Neur.*, **163**, 81-106, 1975.

Gold, M.R. and Martin, A.R., "Inhibitory conductance changes at synapses in the lamprey brainstem", *Science*, **221**, 85-87, 1983.

Goldstein, S.S. and Rall, W., "Changes of action potential shape and velocity for changing core conductor geometry", *Biophys. J.*, **14**, 731-757, 1974.

Godfraind, J.M. and Meulders, M., "Effect de la stimulation somatique sur les champs visuels des neurones de la region genouillee chez le chat anesthesie au chloralose", *Exp. Brain Res.*, **9**, 183-200, 1969.

Guillery, R.W., "A study of Golgi preparations from the dorsal lateral geniculate nucleus of the adult cat", *J. comp. Neurol.*, **238**, 21-50, 1966.

Guillery, R.W., "The organization of synaptic interconnections in the laminae of the dorsal lateral geniculate nucleus of the cat", *Z. Zellforsch.*, **96**, 1-38, 1969a.

Guillery, R.W., "A quantitative study of synaptic interconnections in the dorsal lateral geniculate nucleus of the cat", *Z. Zellforsch.*, **96**, 39-48, 1969b.

Hamori, J., Pasik, T., Pasik, P. and Szentagothai, J., "Triadic synaptic arrangements and their possible significance in the lateral geniculate nucleus of the monkey", *Brain Res.*, **80**, 379-393, 1974.

Hamos, J.E., Raczkowski, D., van Horn, S.C. and Sherman, S.M., "The ultrastructural substrates for synaptic circuitry of an X retinogeniculate axon", *Neurosci. Abst.* **9**, 814, 1983.

Hamos, J.E., van Horn, S.C., Raczkowski, D., Uhrich, D.J. and Sherman, S.M., "Input and output organization of a local circuit neuron in the cat's lateral geniculate nucleus", *Neurosci. Abst.* **10**, 1984.

Helmholtz, H. von., *Handbuch der physiologischen Optik*, 1866. Translated by J.P. Southall, New York, Dover, 1925.

Herz, A., Creutzfeldt, O. and Fuster, J., "Statistische Eigenschaften der Neuronenaktivitat im ascendierenden visuellen System", *Kybernetik*, **2**, 61-71, 1964.

Hoffman, K.-P., Stone, J. and Sherman, S.M., "Relay of receptive-field properties in dorsal lateral geniculate nucleus of the cat", *J. Neurophysiol.*, **35**, 518-531, 1972.

Hubel, D.H. and Wiesel, T.N., "Integrative action of the cat's lateral geniculate body", *J. Physiol.*, **155**, 385-398, 1961.

Hughes, H.C. and Mullikin, W.H., "Brainstem afferents to the lateral geniculate nucleus of the cat", *Exp. Brain Res.*, **54**, 253-258, 1984.

Jack, J.J., Noble, D. and Tsien, R.W., *Electric current flow in excitable cells*. Oxford, Clarendon Press, 1975.

Jahnsen, H. and Llinas, R., "Electrophysiological properties of guinea-pig thalamic neurones: an *in vitro* study", *J. Physiol.*, **349**, 205-226, 1984a.

Jahnsen, H. and Llinas, R., "Ionic basis for the electroresponsiveness and oscillatory properties of guinea-pig thalamic neurones *in vitro*", *J. Physiol.*, **349**, 227-247, 1984b.

Jones, E.G. and Powell, T.P.S., "Morphological variations in the dendritic spines of the neocortex", *J. Cell Sci.*, **5**, 509-529, 1969a.

Jones, E.G. and Powell, T.P.S., "An electron microscopic study of the mode of termination of cortico-thalamic fibres within the sensory relay nuclei of the thalamus", *Proc. R. Soc. Lond. B*, **172**, 173-185, 1969b.

Kemp, J.A. and Sillito, A.M., "The nature of the excitatory transmitter mediating X and Y cell inputs to the cat dorsal lateral geniculate nucleus", *J. Physiol.*, **323**, 377-391, 1982.

Koch, C., "Nonlinear information processing in dendritic trees of arbitrary geometry", *Ph.D. Thesis*, University of Tübingen, 1982.

Koch, C. and Poggio, T., "A theoretical analysis of electrical properties of spines", *Proc. R. Soc. Lond. B*, **218**, 455-477, 1983a.

Koch, C. and Poggio, T., "Electrical properties of dendritic spines", *Trends Neurosci.*, **6**, 80-83, 1983b.

Koch, C. and Poggio, T., "A Simple Algorithm for Solving the Cable Equation in Dendritic Trees of Arbitrary Geometry", *J. Neurosci. Methods*, Submitted, 1984.

Koch, C., Poggio, T. and Torre, V., "Retinal ganglion cells: a functional interpretation of dendritic morphology", *Phil. Trans. R. Soc. Lond. B*, **298**, 227-264, 1982.

Koch, C., Poggio, T. and Torre, V., "Nonlinear interactions in a dendritic tree: localization, timing, and role in information processing", *Proc. Natl. Acad. Sci. USA*, **80**, 2799-2802, 1983.

Koch, C. and Ullman, S., "Selecting one among the many: a simple network implementing shifts in selective visual attention", *Artificial Intelligence Lab. Memo*, No. 723, MIT, Cambridge, 1984.



- LeVay, S. and Ferster, D., "Proportions of interneurons in the cat's lateral geniculate nucleus", *Brain Res.*, **164**, 304-308, 1979.
- Lin, C.-S., Kratz, K.E. and Shermna, S.M., "Percentage of relay cells in the cat's lateral geniculate nucleus", *Brain Res.*, **131**, 167-173, 1977.
- Lindstrom, S., "Synaptic organization of inhibitory pathways to principal cells in the lateral geniculate nucleus of the cat", *Brain Res.*, **234**, 447-453, 1982.
- Livingstone, M.S. and Hubel, D.H., "Effects of sleep and arousal on the processing of visual information in the cat", *Nature*, **291**, 554-561, 1981.
- Llinas, R. and Jahnsen, H., "Electrophysiology of mammalian thalamic neurones *in vitro*", *Nature*, **297**, 406-408, 1982.
- Llinas, R. and Yarom, Y., "Properties and distribution of ionic conductances generating electroresponsiveness of mammalian inferior olivary neurones *in vitro*", *J. Physiol.*, **315**, 569-584, 1981.
- MacKay, D.M., "Elevation of visual threshold by displacement of retinal image", *Nature*, **225**, 90-92, 1970.
- Meulders, M. and Godfraind, J.M., "Influence du reveil d'origine reticulaire sur l'entendue des champs visuels des neurones de la region genouille chez le chat avec cerveau intact ou avec cerveau isole", *Exp. Brain Res.*, **9**, 201-220, 1969.
- Macchi, G. and Rinvik, E., "Thalamo-telencephalic circuits: a neuroanatomical survey", In: *Handbook of Electroencephalography and Clinical Neurophysiology*, Vol. 2(A), Ed. O. Creutzfeldt, Elsevier, Amsterdam, 1976.
- Maffei, L. and Fiorentini, A., "The visual cortex as a spatial frequency analyser", *Vision Res.*, **13**, 1255-1267, 1973.
- McCarley, R.W., Benoit, O. and Barrionuevo, G., "Lateral geniculate nucleus unitary discharge in sleep and waking: state- and rate-specific aspects", *J. Neurophysiol.*, **50**, 798-817, 1983.
- Mcllwain, J.T. and Creutzfeldt, O.D., "Microelectrode study of synaptic excitation and inhibition in the lateral geniculate nucleus of the cat", *J. Neurophysiol.*, **30**, 1-21, 1967.
- Miller, R.F., "The neuronal basis of ganglion-cell receptive-field organization and the physiology of amacrine cells". In: *The Neurosciences: Fourth Study Program*, Eds. F.O. Schmitt and F.G. Worden, MIT Press, Cambridge, 1979.
- Minderhoud, J.M., "An anatomical study of the efferent connections of the thalamic reticular nucleus", *Exp. Brain Res.*, **12**, 435-446, 1971.

Nakai, Y. and Takaori, S., "Influence of norepinephrine-containing neurons derived from the locus coeruleus on lateral geniculate neuronal activities of cats", *Brain Res.*, **71**, 47-60, 1974.

Noda, H., "Depression in the excitability of relay cells of lateral geniculate nucleus following saccadic eye movements in the cat", *J. Physiol.*, **249**, 87-102, 1975a.

Noda, H., "Discharges of relay cells in lateral geniculate nucleus of the cat during spontaneous eye movements in light and darkness", *J. Physiol.*, **250**, 579-595, 1975b.

Oertel, W.H., Graybiel, A.M., Mugnaibi, E., Elde, R.P., Schmechel, D.E. and Kopin, I.J., "Coexistence of glutamic acid decarboxylase- and somatostatin-like immunoreactivity in neurons of the feline nucleus reticularis thalami", *J. Neurosci.*, **3**, 1322-1332, 1983.

Ohara, P.T., Lieberman, A.R., Hunt, S.P. and Wu, J.-Y., "Neural elements containing glutamic acid decarboxylase (GAD) in the dorsal lateral geniculate nucleus of the rat: immunohistochemical studies by light and electron-microscopy", *Neurosci.*, **8**, 189-211, 1983.

Ohara, P.T., Sefton, A.J. and Lieberman, A.R., "Mode of termination of afferents from the thalamic reticular nucleus in the dorsal lateral geniculate nucleus of the rat", *Brain Res.*, **197**, 503-506, 1980.

Parnas, I. and Segev, I., "A mathematical model for conduction of action potentials along bifurcating axons", *J. Physiol.*, **295**, 323-343, 1979.

Posner, M.I., Cohen, Y. and Rafal, R.D., "Neural systems control of spatial orienting", *Phil. Trans. R. Soc. Lond. B*, **298**, 187-198, 1982.

Rall, W., "Time constants and electrotonic length of membrane cylinders and neurons", *Biophys. J.*, **9**, 1483-1508, 1969.

Rall, W., "Core conductor theory and cable properties of neurons". In: *Handbook of physiology*, Vol. 1, Eds. E. Kandel and S. Geiger, American Physiological Society, Washington, D.C., 1977.

Ralston, H.J., "Evidence for presynaptic dendrites and a proposal for their mechanism of action", *Nature*, **230**, 585-587, 1971.

Rapisardi, S.C. and Miles, T.P., "Synaptology of the retinal afferent in the cat lateral geniculate nucleus", *J. comp. Neurol.*, **223**, 515-534, 1984.

Richards, W., "Spatial remapping in the primate visual system", *Kybernetik*, **4**, 146-156, 1968.

Richter, J. and Ullman, S., "A model for the temporal organization of X- and Y-type receptive fields in the primate retina", *Biol. Cybern.*, **43**, 127-145, 1982.

- Riggs, L.A., Merton, P.A. and Morton, H.B., "Suppression of visual phosphenes during saccadic eye movements", *Vision Res.*, **14**, 997-1011, 1974.
- Scheibel, M.E. and Scheibel, A.B., "On the nature of dendritic spines. Report of a workshop", *Commun. Behav. Biol. A*, **1**, 231-265, 1968.
- Schmielau, F., "Integration of visual and nonvisual information in nucleus reticularis thalami of the cat". In: *Developmental neurobiology of vision*, Ed. R.D. Freeman, Plenum Press, New York, 1979.
- Schmielau, F. and Singer, W., "The role of visual cortex for binocular interactions in the cat lateral geniculate nucleus", *Brain Res.*, **120**, 354-361, 1977.
- Segev, I. and Parnas, I., "Synaptic integration mechanisms", *Biophys. J.*, **41**, 41-50, 1983.
- Segev, I. and Rall, W., "Theoretical analysis of neuron models with dendrites of unequal electrical lengths", *Neurosci. Abst.*, **9**, 102.20, 1983.
- Sherman, S.M., "Parallel pathways in the cat's geniculocortical system: W-, X-, and Y-cells". In: *Changing concepts of the nervous system*, Eds. A.R. Morrison and P.L. Strick, Academic Press, New York, 1982.
- Sherman, S.M., "Functional organization of the W-, X-, and Y-cell pathways in the cat: a review and hypothesis", In: *Progress in Psychobiology and Physiological Psychology*, Eds. J.M. Sprague and A.N. Epstein, Academic Press, New York, 1984.
- Sherman, S.M. and Spear, P.D., "Organization of visual pathways in normal and visually deprived cats", *Physiol. Rev.*, **62**, 738-855, 1982.
- Shapley, R.M. and Hochstein, S., "Visual spatial summation in two classes of geniculate cells", *Nature*, **256**, 411-413, 1975.
- Sillito, A.M. and Kemp, J.A., "The influence of GABAergic inhibitory processes on the receptive field structure of X and Y cells in the cat dorsal lateral geniculate nucleus (dLGN)", *Brain Res.*, **277**, 63-77, 1983.
- Sillito, A.M., Kemp, J.A. and Berardi, N., "The cholinergic influence on the function of the cat dorsal lateral geniculate nucleus (dLGN)", *Brain Res.*, **280**, 299-307, 1983.
- Singer, W., "The effect of mesencephalic reticular stimulation on intracellular potentials of cat lateral geniculate neurons", *Brain Res.*, **61**, 35-54, 1973.
- Singer, W., "Control of thalamic transmission by corticofugal and ascending reticular pathways in the visual system", *Physiol. Rev.*, **57**, 386-420, 1977.
- Singer, W. and Bedworth, N., "Inhibitory interaction between X and Y units in the cat lateral geniculate nucleus", *Brain Res.*, **49**, 291-307, 1973.

Singer, W. and Bedworth, N., "Correlation between the effects of brain stem stimulation and saccadic eye movements on transmission in the cat lateral geniculate nucleus", *Brain Res.*, **72**, 185-202, 1974.

Singer, W. and Creutzfeldt, O.D., "Reciprocal lateral inhibition of On- and Off-Center neurones in the lateral geniculate body of the cat", *Exp. Brain Res.*, **10**, 311-330, 1970.

Singer, W., Poppel, E. and Creutzfeldt, O., "Inhibitory interaction in the cat's lateral geniculate nucleus", *Exp. Brain Res.*, **14**, 210-226, 1972.

Sloper, J.J. and Powell, T.P.S., "An experimental electron microscopic study of afferent connections to the primate motor and somatic sensory cortices", *Phil. Trans. R. Soc. Lond. B*, **285**, 199-226, 1979.

So, Y.T. and Shapley, R., "Spatial properties of X and Y cells, in the lateral geniculate nucleus of the cat and conduction velocities of their inputs", *Exp. Brain Res.*, **36**, 533-550, 1979.

Sterling, P and Davis, T.L., "Neurons in the cat lateral geniculate nucleus that concentrate exogenous [<sup>3</sup>H]γ-amino butyric acid (GABA)", *J. comp. Neurol.*, **192**, 737-749, 1980.

Torre, V. and Poggio, T., "A synaptic mechanism possibly underlying directional selectivity to motion", *Proc. R. Soc. Lond. B*, **202**, 409-416, 1978.

Tsumoto, T., Creutzfeldt, O.D. and Legendy, C.R., "Functional organization of the corticofugal system from visual cortex to lateral geniculate nucleus in the cat", *Exp. Brain Res.*, **32**, 345-364, 1978.

Tsumoto, T. and Suzuki, D.A., "Effects of frontal eye field stimulation upon activities of the lateral geniculate body of the cat", *Exp Brain Res.*, **25**, 291-306, 1976.

Wassle, H., Boycott, B.B. and Illing, R.-B., "Morphology and mosaic of on- and off-beta cells in the cat retina and some functional considerations", *Proc. R. Soc. Lond. B*, **212**, 177-195, 1981.

Wassle, H., Peichl, L. and Boycott, B.B., "Morphology and topography of on- and off-alpha cells in the cat retina", *Proc. R. Soc. Lond. B*, **212**, 157-175, 1981.

Wilson, J.R., Friedlander, M.J. and Sherman, S.M., "Fine structural morphology of identified X- and Y-cells in the cat's lateral geniculate nucleus", *Proc. R. Soc. Lond. B*, In press, 1984.

Wong, M.T.T., "Somato-dendritic and dendro-dendritic synapses in the squirrel monkey lateral geniculate nucleus", *Brain Res.*, **20**, 135-139, 1970.

Yingling, C.D. and Skinner, J.E., "Gating of thalamic input to cerebral cortex by nucleus reticularis thalami". In: *Attention, voluntary contraction and event-related cerebral potentials. Prog. Clin. Neurophysiol.*, 1, Ed. J.E. Desmedt, Karger, Basel, 1977.